

Estimation and inter-comparison of dust aerosols based on MODIS, MISR and AERONET retrievals over Asian desert regions

Ammara Habib^{1,2}, Bin Chen,^{1,2,3,} Bushra Khalid,^{1,2,4,5} Saichun Tan^{1,3}, Huizheng Che⁶, Tariq Mahmood^{1,2,7}, Guangyu Shi^{1,2}, Yasunobu Iwasaka⁸, Muhammad Tahir Butt⁹*

1. *Institute of Atmospheric Physics, Chinese Academy of Sciences, Beijing 100029, China*
2. *University of Chinese Academy of Sciences, Beijing 100049, China*
3. *Collaborative Innovation Center on Forecast and Evaluation of Meteorological Disasters, Nanjing University of Information Science & Technology, Nanjing, 210044, China.*
4. *International Institute for Applied Systems Analysis, Laxenburg, Austria.*
5. *Department of Environmental Science, International Islamic University, Islamabad, 46300, Pakistan*
6. *Key Laboratory of Atmospheric Chemistry (LAC), Institute of Atmospheric Composition, Chinese Academy of Meteorological Sciences (CAMS), CMA, Beijing, 10081 China.*
7. *Pakistan Meteorological Department, Islamabad, Pakistan*
8. *Kanazawa Univeristy, Kakoma , Kanazawa, Japan.*
9. *Center for Environmental Protection Studies, PCSIR Laboratories Complex, Lahore, Pakistan*

● Correspondence. E-mail: chen_bin@mail.iap.ac.cn (Bin Chen)

Abstract

This study presents detailed analysis of spatiotemporal variations and trend of dust optical properties i.e., Aerosol Optical Depth (AOD) and Angstrom component over Asian desert regions using thirteen years data (i.e., 2001-2013) retrieved from Aerosol Robotic Network (AERONET), Moderate Resolution Imaging Spectroradiometer (MODIS) and Multi-angle Imaging Spectroradiometer (MISR). These regions include Solar Village, Dunhuang and Dalanzadgad and are considered as origin of desert aerosols in Asia. Mann Kendall trend test was used to show the trend of AOD. The relationship of AOD with weather parameters and general AOD trend over different wavelengths has also been shown. AOD's trend has been observed significant throughout the year in Solar Village, while in Dunhuang and Dalanzadgad the significant trend has been found only in peak period (March –June). Analysis show high values of AOD and low values of angstrom in Solar Village during peak period. In Chinese desert regions high values of AOD have been found during peak period and low values in pre peak period. Significant relationship has been observed between AOD and average temperature in Solar Village and Dalanzadgad whereas rainfall and wind speed showed no significant impact on AOD in all desert regions.

Keywords: AOD, angstrom exponent, AERONET, MODIS, MISR, desert

1. Introduction

Aerosols in the atmosphere are colloids of solid and liquid particles originating from natural and anthropogenic activities. Natural activities added aerosols include mineral dust from dust storms, volcanic ashes, burning (fires from forests), pollens and sea salt etc. and anthropogenic activities add particulate matter (PM) from fossil fuel combustion and smoke from biomass burning (Kim et al., 2003; Zhang et al., 2010). Aerosols have significant impact on global climate directly by scattering and absorption; indirectly by cloud properties that cause the large uncertainties in radiative forcing measurements.

Aerosols play an important role in analysis and prediction of global climate studies, this is why accurate and reliable measurements are needed to reduce uncertainties (Hansen et al., 2000). Aerosols affect earth's surface temperature by scattering or absorption of short wave radiations (Haywood and Boucher, 2000; Menon et al., 2002). Efforts have been made to improve the aerosol characterization methods by using in situ measurements, ground based measurements, aerosol modeling and satellite measurements (Chen et al., 2015; Kahn et al., 2005). Satellites provide repeated global coverage and have substantial advantage of synoptically mapping of vast area in a single image while ground based measurements usually limited to spatial coverage (Kosmopoulos et al., 2008). To investigate the aerosol distributions along with its physical, chemical and optical properties, integrating the ground-based data

with satellite data in order to interpret it in a comprehensive context, aerosol transport models have become more critical.

Aerosol optical depth is an indication of the amount of aerosols in the vertical column of aerosol loading in the atmosphere, considered as one of the primary optical properties of aerosols (Prasad and Singh, 2007). Numerous studies have been carried out regarding the aerosols optical properties, spatial and temporal distribution of aerosols and their impact on atmospheric radiation and climate (Kaufman et al., 1997; Vinoj, 2004; Chen, 2015). AERONET (Aerosols Robotic Network) is a sky scanning and sun robotic measurement programme that has developed rapidly since 1993 and has launched hundreds of sites all over the world. In addition to the ground based networks, multi satellites such as the MODIS and MISR provide aerosol optical retrievals across the globe (Sayer et al., 2013). Ground based measurements of dust aerosols provide significant and most reliable hourly information of physical and optical properties of dust at strategic locations (Holben et al., 1998). It is believed that precipitation patterns and regional temperature influence the aerosol loading in Chinese regions since 1970s with direct and indirect impacts (Li et al., 2007).

Chinese and Mongolian deserts are significant source of mineral dust in Asian region. During spring season this Asian dust is transported by Westerlies over thousands of kilometers (Iwasaka et al., 2004). Many researchers have studied AOD properties retrieved from satellite datasets (Mishchenko and Geogdzhayev, 2007; Zhang Y, 2010). Li et al. (2014) studied long term trend of aerosol optical properties based on AERONET measurements over 90 stations in North America, South Africa, Europe and Asia. The Intercomparison studies of MODIS, MISR and GOCART products against AERONET conducted by Cheng et al. (2012) from 2001-2011 over four sites in China and four sites of the Europe, USA and North Africa.

In south west Asian regions, Arabian Peninsula located in subtropical belt has also been considered as a major source of desert dust (Edgell, 2006). Solar Village is an important continental remote area in Saudi Arabia considered as a major source of desert aerosols in this region. In pre-monsoon season, the westerly winds from arid regions bring dust aerosols and are the cause of dust storms (Miller et al., 2008). The continuous outbreaks of dust events not only impact atmospheric environment in downwind areas but also is a major cause of aerosol concentration in source regions. It is revealed from satellite remote sensing and ground based measurements that in Asian desert regions maximum aerosol loading has been found during spring season (Zhang et al., 2003). However, spatial and temporal distribution of dust retrievals is still limited for the Asian desert regions.

Several studies have been conducted during the last decade in Saharan region, which is the most active contributor and largest dust source in the world. Ground based measurements from AERONET during Safari campaign in the year 2000 were used to compare with MODIS and MISR based satellite retrievals

by Diner et al., (2001). Dust aerosol climatology over South Africa on seasonal basis using MISR data for the period of 10 years has been reported by Tesfaye et al. (2011). Kumar et al. (2014), conducted a comprehensive study on long term (i.e., 2003-2013) trends and variations in aerosol optical depth parameters retrieved from MODIS over three stations of South Africa. Several studies have been published regarding aerosol optical depth and Angstrom exponent in North West China using ground based observations (Kumar et al., 2014; Xiangao et al., 2004; Yu et al., 2015). The Intercomparison of MODIS AOD and MISR AOD against AERONET AOD have not been conducted yet in Asian dust regions. The information on the relationship of AOD with meteorological parameters is also limited in the scientific literature for Asian dust regions. This study focuses to fill the aforementioned gap. This study investigates the inter-seasonal variability in Asian dust regions during pre-peak period, peak period and post peak period.

In the present study, level-3 aerosol data collection 6 retrieved from MODIS-Terra sensor and MISR level-3 data has been considered against AERONET data level 2.0 of aerosol optical properties for the study period of 2001-2013 over Asian desert regions. The objective of this study is to analyze the dust optical properties based on various platforms, their trends and relationship with weather parameters in Asian desert regions. First, we estimated trend of AOD and Angstrom Exponent (α) based on monthly averages data set for the years 2001-2013. Further, we have analyzed the variability of AOD and Angstrom Exponent against meteorological parameters. Finally, we compared MODIS and MISR data against AERONET and meteorological parameters such as temperature, rainfall and wind speed.

2. Study area, data and analysis

AOD and Angstrom Exponent were measured for three different locations i.e., Dunhuang (40.1421° N, 94.6620° E) located in northwest edge of Taklamakan desert, Dalanzadgad (43.5685° N, 104.4141° E) located in the territory of eastern part of Gobi Desert, and Solar Village (24.91° N, 46.41° E) located 30 km northwest of Riyadh, Saudi Arabia. To study AOD and AE, detailed trend and variability, we divided data into pre peak period (Nov, Dec, Jan, Feb), peak period (March, April, May, June) and post peak period (July, Aug, Sep, Oct). The peak periods have been determined on the basis of aerosol response in different seasons on similar lines as discussed by Wang et al., (2011). The present research is carried out using MODIS, MISR and AERONET data to compare desert aerosol loadings and trend over three Asian desert regions (i.e., Dalanzadgad, Dunhuang and Solar Village) for the period of 13 years i.e., 2001-2013. We compared satellite observations (i.e., MISR & MODIS) with ground based observations i.e., AERONET in the study regions to validate the AOD and Angstrom Exponent. The CRU ts 2.3 at 0.75° spatial resolution data was downloaded for total monthly rainfall (mm) and average monthly temperature (°C). Re-Analysis Interim (ERA-interim) at 0.75° resolution data was used for Average Meridional Wind speed (m/sec). To

study 13 year trend of aerosols, Mann-Kendall trend analysis (MK Test) was considered based on monthly averaged AOD and Angstrom Exponent over Asian desert regions. Spatial correlation has been computed between multi-satellite dataset against AERONET and meteorological parameters.

2.1 AERONET

AERONET is a well-organized ground based robotic network of more than 300 sites around the globe which use sky radiometer and sun photometer for aerosol measurements (Holben et al., 1998). The spectral ranges for direct sun between 340–1020 nm and diffuse sky 440–1020 nm radiances are employed by sun-photometer to take AERONET measurements. The AERONET provides AOD with low uncertainty ± 0.01 for wavelength > 440 nm and ± 0.02 for shorter wavelengths and globally used to validate satellite AOD retrieved values (Holben et al., 1998). In this study, we have used the Level 2.0 Version 2 data products which is quality assured and cloud screened (Smirnov et al., 2000). To study long term trend or aerosol optical properties we selected AERONET stations over desert sites based on the availability of long term data sets. The AERONET data products were downloaded from <http://aeronet.gsfc.nasa.gov>. Data was missing in year 2008 in pre peak period, 2008-2009 in peak period and 2007-2010 during post peak period in Dalanzadgad desert region. Data has been considered and analysis has been performed on the basis of data availability.

2.2 MODIS

MODIS instrument has been flying aboard Terra is an important part of NASA Earth Observing System since December 1999. It provides data on number of aerosol products for ocean and land (Kaufman et al., 1997). MODIS sensor measures radiances at spatial resolutions of 0.25, 0.5 and 1.0 km. It has 36 spectral channels from 0.415 to 14.235 μm with a viewing swath of 2330 km. To retrieve aerosol optical properties over brighter targets (deserts and urban areas) deep blue algorithm has been used (Hsu et al., 2012). Over land MODIS AOD uncertainty is 0.05 ± 0.15 (Kaufman et al., 1997). In this study aerosol data MODIS Terra collection 6 has been used with spatial resolution of $1^\circ \times 1^\circ$ retrieved from MODIS sensor and downloaded from <http://disc.sci.gsfc.nasa.gov/giovanni> website.

2.3 MISR

MISR onboard Terra with nine cameras, has 4 spectral bands i.e., green, blue, red and near infrared (Diner et al., 1998). The coverage time around globe is nine days with recurrence coverage between two and nine depending upon latitude. In this study we used level two AOD products over land obtained at $0.5^\circ \times 0.5^\circ$ downloaded from <http://disc.sci.gsfc.nasa.gov/giovanni> website. The MISR data AOD uncertainty is 0.05 ± 0.2 AOD. MODIS-MISR correlation studies have been reported in the past (Kahn et al., 2009; Shi et al., 2011; Xiao et al., 2009). The MISR data $0.5^\circ \times 0.5^\circ$ has been rescaled to $1^\circ \times 1^\circ$ degrees resolution. The

equal weight has been assigned to perform rescaling to each sub grid and $1^\circ \times 1^\circ$ grid has been obtained. It considered valid only when more than half of sub-grids have valid data.

2.4 MODIS and MISR validation against AERONET

AERONET measurements are considered as most effective tool to validate satellite AOD (Levy et al., 2010). In the present study, level 2.0 sun photometer retrieved AOD₅₀₀ data were acquired from AERONET sites in Dalanzadgad and Solar Village for the period of 2002-2013. Spatial monthly averaged data of MODIS and MISR AOD were compared to AERONET with temporal monthly averaged AERONET AOD data. The spatial and temporal averages of AOD and sun photometer AODs of MODIS, MISR respectively were compared.

The AODs from MODIS and MISR were retrieved at 550–555 nm respectively while the nearest sun photometer AODs frequency was recovered at 500 nm. For the purpose of direct comparison and validation of AOD at 550 nm, the Angstrom Exponent is calculated between 440 and 870 nm for retrieving AERONET AOD at 550 nm, for determining a common wavelength for both satellites and AERONET, the following equation was used (Kumar et al., 2015; Prasad and Singh, 2007).

$$AOD_{550} = AOD_{500} (550/500)^{-\alpha}$$

Where α is the (440- 870 nm) Angstrom exponent and AOD₅₀₀ is aerosol optical depth at 500nm.

The MK trend test is a statistical tool used to identify the existence of monotonic trend in time series (Kendall, 1975; Mann, 1945). The MK test is nonparametric test which has been commonly used to detect trend in climatological studies (Chattopadhyay et al., 2012; Yue et al., 2002).

To determine real slope of MK trend research Sen's Slope estimator is used (Gilbert, 1987; Sen, 1968). We have used the MK test to determine the trend of AOD and Angstrom exponent in all study regions at 0.05 significance level. Two hypotheses factors (H_0 and H_1) were computed by MK test, where H_0 is no trend in the time series/There is no relationship between variables and H_1 is trend in the time series/There is relationship between variables

This test is applied on all observed data sets of AOD and Angstrom Exponent to see the general trend of these two variables in Dalanzadgad, Dunhuang and Solar Village from AERONET, MODIS and MISR retrieval data.

2.5 Linear regression

Linear regression analysis as described by (Tripathi et al., 2005) was applied for AOD from MODIS, MISR and AERONET with meteorological parameters as Eq. (2).

$$AOD_{\text{satellite}} = m \times AOD_{\text{AERONET}} + c \quad (2)$$

Where, c is intercept; m is slope. $AOD_{\text{satellite}}$ illustrates AOD from MODIS and MISR satellites. R^2 is defined as the coefficient of determination or square of correlation coefficient that represents the correlation between AOD from AERONET MODIS, MISR with meteorological parameters. .

3. Results and discussions

3.1 Aerosol optical depth and angstrom exponent trend analysis

MK test is applied to observe the trend of AERONET AOD in Dalanzadgad and Solar Village over period of 2001-2013. The results of MK test analysis are illustrated in **Table 1**. The significant trend of AERONET AOD has been observed in Dalanzadgad desert region in pre peak period whereas insignificant trends have been observed in peak and post peak periods for AERONET dust retrievals in this region (**Table 1, Fig. 1**). Significant trend of AERONET AOD has been observed in Solar Village in pre peak period, peak period and post peak period (**Table 1**).

Table 2 presents the trend of MODIS AOD in Dalanzadgad, Dunhuang and Solar Village. In Dalanzadgad, significant trend has been observed in pre peak period whereas insignificant trend has been found in peak and post peak periods (supporting material **Fig. S 1-4**). In Dunhuang significant trend has been observed only in peak period whereas insignificant trend has been found in pre peak and post peak periods (**Table 2**).

In Solar Village insignificant trend of MODIS AOD has been observed in pre peak period whereas significant trend has been found in peak and post peak periods. This result of Solar Village MODIS AOD strongly agrees with our AERONET AOD results. The presence of trend in post peak period shows the high dust activity during these months.

Table 3 presents trends of MISR AOD in Dalanzadgad, Dunhuang and Solar Village. No significant trend of MISR AOD has been found in Dalanzadgad Solar Village and Dunhuang MK trend analysis of AERONET AE has been shown **Table 4**. No significant trend of Angstrom Exponent found in all the three periods (i.e., pre peak period, peak period and post peak period) in all study areas (See supporting material). MK trend analysis of MODIS AE illustrated in Table 5 in Dunhuang and Solar Village for all periods. No trend of AE has been found in Dalanzadgad in pre peak period, peak period and post peak period.

Many researchers reported the long term trend of AERONET AOD on regional scale and worldwide (Li et al., 2015; Xia, 2011; Yoon et al., 2012). AOD trend retrieved from multiple sensors have been found decreasing over the Western Europe and US and increasing over the Indian Subcontinent, Middle East and some parts of China. Significant increasing trend of AERONET retrieved AOD has been found in Solar Village by Li et al., (2014). In this study, significant seasonal increasing trend of AOD has been found in China during March to May (MAM) and June to August (JJA), which could be due to high dust uplifting activities from desert of Mongolia and China. The decreasing trends of seasonal AOD have been reported in

China during September to November (Ogunjobi et al., 2003; Park et al., 2010). In Northern hemisphere, the AOD trends are mostly prominent in spring (MAM) and summer (JJA) seasons (Li et al., 2014). High AOD values have been found by many researchers in other Chinese deserts as well i.e., Taklamakan desert from April to August. This high AOD value may be due to the up lifting of dust aerosols and occurrence of coarse mode aerosols which is the greatest contributor of back ground Asian dust in Taklamakan desert (He et al., 2016; Ogunjobi et al., 2003). Increasing trend of AOD has been investigated in economically growing areas of Asian region (India and China) and Arabian Peninsula (Mehta et al., 2016). The high AOD values have been verified by satellite observation and model results at Solar Village (Chin et al., 2014; Hsu et al., 2012). AERONET data further validated that negative trend in AE in Solar village is due to increased dust emissions in this region (Li et al., 2014).

3.2 Aerosol optical depth variability and its relation to the meteorological parameters

3.2.1 Dalanzadgad

Fig. 2 (a-c) presents the monthly averaged AOD variability in Dalanzadgad retrieved from AERONET, MODIS and MISR at from 2001-2013. The wavelength 550 nm has been considered for ground and satellite based observational data as it best corresponds to peak of the solar spectrum and mid visible range where the radiative effect is highest (Floutsi et al., 2016). In pre peak period, monthly averages AERONET AOD were observed to be ranging from 0.04 to 0.12 (**Fig. 2 a**). Aerosol loading has been revealed to be highest during 2010 amongst the 13 years observations monitored for the study through AERONET AOD and MODIS AOD values ranging from 0.05 to 0.18. During the years 2005 and 2011 highest MODIS AOD values have been recorded. MISR derived AOD ranges from 0.05 to 0.12. High AOD values have been recorded in 2003 and 2005. Good agreement has been found between MODIS and MISR AOD in Dalanzadgad pre peak period in 2005. During peak period, monthly averages AERONET AOD ranged from 0.07 to 0.21 (**Fig. 2 b**). Aerosol loading has been revealed to be highest during 2003 amongst the 13 years of observations recorded for the study through AERONET AOD. MODIS retrieved AOD values ranging from 0.14 to 0.26. During the years 2001, 2003, 2008 and 2010 highest (> 0.2) MODIS AOD values have been recorded. MISR derived AOD ranges from 0.14 to 0.26. High AOD values have been recorded in 2003, 2006, 2008 and 2011 (> 0.2). No significant agreement has been observed in the studied observations during the 13-year period for AERONET, MODIS and MISR except for the year of 2003 which has shown highest AOD during the peak period in all the three datasets. Although there is a difference in the AOD values observed through the three datasets even for the year of 2003. In the post peak period, monthly average of AERONET AOD ranges from 0.05 to 0.12 (**Fig. 2 c**). Aerosol loading has been revealed highest during 2002 in the post peak period of concentration whilst 4 years data (from 2007 to 2010) was missing on data sources amongst the 13 years of observations recorded for the study with AERONET AOD.

Fig. 2 d illustrates the meteorological parameters in Dalanzadgad from 2001-2013. Rainfall data more than 2 mm/month has been observed during 2003, 2006, 2011, 2012 and 2013 in comparison to the 13 years of study observations. Lower temperature (i.e., 10°C) has been recorded for 6 years i.e., 2003, 2005 and from 2008-2012. High wind speed (i.e., 1.2 m/sec) has been observed in year 2004. From the observations it has been revealed that meteorological parameters like lower temperature, high rainfall rates and high wind velocities are directly related to the aerosol distribution and aerosol loading in Dalanzadgad. **Fig. 2 e** illustrates the meteorological parameters in Dalanzadgad from 2001-2013 during the peak period. Average rainfall has been observed more than 10 mm/month during 2002, 2004, 2008, 2010, 2011 and 2012 and has been recorded to be exceedingly high during 2003 i.e., 22 mm/month. The temperature ranges between 2.6°C-16.5°C during the 13 years of peak period with the highest temperature i.e., 16.5°C recorded for the year of 2006 and the lowest i.e., 2.5°C for the years of 2003 and 2007. Wind speed (> 1.2 m/sec) has been recorded for the year of 2005, 2006, 2007 and 2011 while velocity (< 1 m/sec) has been observed during 2009 and 2013. From the observations it has been noted that meteorological parameters like lower temperature, high rainfall rates and high wind velocities directly affects the aerosol distributions. **Fig. 2 f** presents the meteorological parameters in Dalanzadgad from 2011-2013. High rainfall has been recorded during 2012 and 2007, whereas average monthly temperature ranges between 14-15°C during post peak period. Wind speed has also been observed very low usually and no significant relationship exists between meteorological parameters and AOD during post peak period.

3.2.2 Solar Village

During the years 2009-2011 AERONET AOD has shown the highest aerosol loading during the 13 years study period while MODIS AOD has shown highest aerosol concentration during 2006-2009. MISR AOD has the highest aerosol concentration in 2011-2012 during the pre-peak period. The three data sources have not shown any agreement in the number of years showing high aerosol concentrations except for the two dataset for the year of 2011. The varying aerosol trend has been shown during the study period through three data sources. With AERONET AOD the aerosol concentration has been found with high aerosol loading during the years 2007-2009 and 2011-2012 and for MODIS AOD data in the years 2008-2009 and 2012 while for MISR AOD in the years 2005, 2008, 2009 and 2012 have excessively high rates of aerosol concentrations during the peak period. The years of 2008, 2009 and 2012 have shown agreement for aerosol loading from all the three data sources for monitoring aerosols concentration. For the post peak period, to monitor aerosol loading, AERONET AOD and MISR AOD have shown agreement in aerosol concentrations during the years 2008, 2010 and 2011 with a concurrence in the loading rates as well but AERONET and MODIS have shown variability in the aerosol concentrations as compared to the other two data sources during the same years (supporting material **Fig. S 5 a-c**).

AOD has been observed highest in the year 2011 for AERONET AOD during the pre-peak period. This may be attributed to the fact that the year of concern had relatively high mean monthly rainfall as observed by the analysis of CRU dataset which still does not clearly link up between the aerosol loading and other meteorological parameters. While trying to figure out the link between aerosol concentration through AERONET data sources and meteorological parameters, no significant connection could be developed in the observed values during the pre-peak period of the 13 years of study. The meteorological parameters like relatively reduced wind speed i.e., 0.85 (m/sec) and low rainfall i.e., 6.67 (mm/month) shows agreement with the aerosol loading during the year of 2009 with the aerosols values obtained from AERONET AOD and MISR AOD. However same cannot be stated for aerosol concentration episode in 2012 during peak period because no correlation could be established between the meteorological factors and loading episodes. AOD during 2008 and 2010 has shown agreement with reduced wind speeds prevalent in the year of concern as compared to other years of study along with less rainfall recorded for the above mentioned years but has not shown significant relevance. The temperature has been recorded about 25 °C with low rainfall and wind speed in post peak period (supporting material **Fig. S 5 d-f**).

3.2.3 Dunhuang

The monthly averages of aerosol concentration and meteorological parameters in Dunhuang have been presented during different periods (supporting material **Fig. S 6 a-c**). It was observed that there was no agreement between MODIS AOD and MISR AOD values for the aerosol concentration during the 13 years in pre peak period. Aerosol concentration observed through MODIS AOD and MISR AOD has not shown agreement during the peak period except for the year of 2003. A dispersed and weak aerosol loading episode during the years 2004 and 2005 observed by MODIS AOD and MISR AOD. The aerosol concentration has been recorded high during the years 2004 and 2005 with MODIS AOD in pre peak period, the difference between the MODIS and MISR AOD is probably due to the uncertainty of satellite retrieval. Mean monthly rainfall has not shown significant impact on aerosol loading during 2003. No significant impact of meteorological parameters on AOD has been found in peak period. The strong relationship can be seen between the aerosol concentrations and the lower values of meteorological parameters during the post peak period in Dunhuang region through 2004 and 2005 years. Similarly, during the years 2007, 2008 and 2009 the excessive increase in rainfall has been observed. These high values may be due to reason of low Angstrom exponent values and high temperature conditions. Higher AOD in Dunhuang desert region and low values of Angstrom Exponent are may be due to the significant dust events over Taklamakan desert region. (Wang et al., 2013) investigated that in the Chinese desert region of Taklamakan, rainfall and wind speed have strongly influenced the dust emissions, transportation, mean average temperature and deposition (supporting material **Fig. S 6 d-f**).

3.3 Angstrom Exponent Variation

AE (α) is a measure of wavelength dependence of AOD and a significant indicator of size distribution of aerosols. **Fig. 3 (a-c)** represents AE retrieved from AERONET and MODIS in pre-peak; peak and post peak period from 2011-2013 in Dalanzadgad desert region. In the pre peak period, high values of AE have been found from AERONET that ranges from 1.5-1.8. In the post peak period values of Angstrom exponent from Aeronet are missing in 2007 and 2008 due to unavailability of data set. In the peak period values from MODIS ranges from 1.1-1.35, and in post peak period high values have been recorded ranging from 1.0-1.07.

For Solar Village, AERONET shows higher values of AE as compared to MODIS during pre-peak, and post peak period ranges from 0.3-0.8. During pre-peak and post peak periods the AE from AERONET ranges from 0.5-0.8 and 0.3-0.7 respectively. The low values of AE have been found in peak period i.e., ranges from 0.1-0.4. The AE values retrieved from MODIS have been found low in comparison to AERONET AE in Solar Village only for the peak period. The values of AE retrieved from MODIS for pre-peak period are 0.5-0.89, peak period 0.1-0.3 and in post peak period 0.3-0.7, are shown in the figures. AE retrieved from MODIS during pre-peak period 0.3-0.5, peak period 0.1-0.3 and post peak period 0.1-0.4 have been observed (supporting material **Fig. S 7 a-c**). In Dunhuang, the MODIS AE during pre-peak period ranges from 0.6-1.4. In peak period the MODIS AE values found between 0.5-0.9 and post peak period, MODIS AE values have been found less 0.2-0.6 (supporting material **Fig. S 8**). High values of AE indicates dominance of fine particles in the study regions whereas low values of Angstrom exponent shows that dust is mainly consist of coarse particles and associated to dust storm events in spring. This change in AE is opposite to that of AOD values. In Dunhuang fine mode dust aerosols are significant in peak and post peak period because of dust activities are predominant during this part of year. High values of AE during peak and post peak period and low value of alpha in Dalanzadgad and Solar Village may possibly by contribution of fine mode aerosols in high temperature period (Lyamani et al., 2006). Tanré et al. (2001) reported the low AE values of desert dust from -1.0 to 0.5 which is in good agreement of presented results. Bi et al. (2011) found the high AE values from July to August over Sacol, which is located on south west edge of Tengger desert area which is considered as significant dust activity area. Gherboudj (2014) studied the seasonal and spatial variation trend of aerosol optical depth 500nm and AE 500-870 in Arabian Peninsula desert regions and in March and September, the Alpha values around 0.4 which is in good agreement of results of peak period in Solar Village.

3.4 Intercomparison of ground based and satellite based AOD with Angstrom Exponent and meteorological parameters

Fig. 4 a, b shows statistically computed spatial correlation between AERONET AOD and AE in Dalanzadgad and Solar Village. Correlations have been found positive for AERONET AOD and AE in

Solar Village than Dalanzadgad and are significant with R value 0.5 and slope 1.2 with RMSE 0.1. A well agreement has also been found between MODIS AOD and AE in Solar Village with R value 0.5, slope with 0.8 and RMSE 0.1 (**Fig. 4 c**). In Dalanzadgad, significant correlation has been found between MODIS AOD and AE with R value 0.4 having slope 1.5 with RMSE 0.1 (**Fig. 4 d**). The relationship of AEROENT AOD with temperature has been found only in Solar Village with $R^2 = 0.2$ having slope with 0.9 x. Considerable agreement has been found between MISR AOD and temperature in Solar Village with R value 0.3 (**Fig. 4 e**). In Dunhuang only relationship has been found between MISR AOD and wind speed m/sec with R^2 value 0.2, slope 0.12 x (**Fig. 4 f**).

No agreement is found in the Dunhuang between AOD and AE (supporting material **Fig. S 9 a**). It means that both coarse mode aerosols and fine mode aerosols are found in the atmosphere at the same time in this region. Negligible correlation has been found between AERONET AOD to MODIS AOD and MISR AOD in Solar village (supporting material **Fig. S 9 b-c**), and in Dalanzadgad **Fig. S 9 (d-e)**. In the Dunhuang, relationship between MISR AOD with temperature has been found insignificant as opposed to that of Solar Village (supporting material **Fig. S 9 f-h**). The relationship of meteorological parameters with AOD has been found negligible in some areas. Negative correlations between AERONET AOD with AODs of MODIS and MISR show that the gaps may occur due to the matching of data points during the study time period or because of the insufficient number of data points. The lower correlation of MODIS in comparison to MISR results may be due to the lower spatial resolution and in consequence to difficulties of MODIS algorithm, when dealing with different aerosol types and surface reflectance.

The exponential dependence of AE in Solar Village and Dalanzadgad by AEROENT AOD and MODIS AOD indicates that aerosols are major contributors of desert dust. AOD increasing with decreasing AE indicates the presence of coarse mode particles. This type of particles mostly originated from local dust events. Che et al. (2013), studied the relationship between the AOD and AE in Taklamakan desert area that coarse particles are significant part of desert aerosols. Prasad and Singh (2007), found poor agreement between AEROENT and MODIS ($R^2 = 0.2$) during summers. Cheng et al. (2012), investigated that China shows lower satellite retrieval accuracy to other sites located in Africa, North America and Europe. MISR sensor, because of its multi-angular characteristics, retrieves AOD better in highly reflective surfaces (Kahn et al., 2010). Christopher et al. (2008), reported that AOD retrievals from MISR sensor is a reliable sensor for AOD data in desert regions with a high correlation value ($R^2 = 0.89$) between AERONET AOD and MISR AOD over different desert regions. Liu et al. (2010), investigated strong correlation ($R^2 = 0.89$) between ground based measurements and MISR AOD in eastern, southwestern and northern parts of China.

4. Conclusions

We used thirteen years data of AOD and AE derived from MODIS and MISR, as well as ground surface measurements of AERONET, evaluated their monthly averaged data, and discussed their trend, seasonal variations compared over Asian desert regions. MK trend analysis shows significant trend of AOD in Solar Village in all three periods, whereas in Dunhuang and Dalanzadgad AOD trend has been shown in peak and post peak periods. MK trend analysis of MODIS AE shows trend only in pre peak period in Solar Village and Dunhuang, however no trend has been observed with AE in all three desert regions. The differences of AOD and Angstrom from different satellites and ground based stations vary from region to region. Moreover, the distributions of AOD found highest values in Solar Village. In Chinese desert regions, the regional monthly means of AOD are high in peak period and low in pre peak period. Low Angstrom Exponent values have been found in Dunhuang and Solar Village, which shows the dominance of coarse particles in these desert regions. A link between optical properties and aerosol production by wind is not easy to detect, the correlation coefficient increases with increasing wind speed; i.e., when there is no wind, a lower correlation coefficient has been found, while wind speed of more than 2 m/s leads to the higher correlation coefficient. A good agreement has been observed between AE and AOD in Solar Village and Dalanzadgad. Regression analysis shows significant relation has been found between wind speed and AOD. The effect of average temperature on the AOD has been found significant in all desert regions. The increase of AOD with increase in temperature has been found in study regions. No significant agreement has been observed between AERONET AOD against MODIS AOD and MISR AOD which may be due to the surface of sensors in different platforms. This may be attributed to large aerosol load and complex aerosol mixtures in desert regions. Variations in meteorological conditions such as rainfall, temperature and wind speed have significantly affected the aerosol concentrations.

Due to the limitations of surface observations, we only have two available AERONET stations data to verify the conclusions. This research work will serve as a reference for evaluating recent trend and variations of dust aerosols over Asian desert regions in future. Further studies will emphasis on combining more satellite and ground based observations over global desert sites to study variation of aerosols and their optical properties.

Acknowledgments

This work was supported by the National Natural Science Foundations of China (Nos. 41475136 and 41590871), the Beijing Open Research Fund of Jiangsu Provincial Meteorological Bureau and International Science & Technology Cooperation Program of China (No. 2013DFG22820).

Appendix A. Supplementary data

Supplementary data associated with this article can be found in the online version.

References

- 1 Bi, J, Huang, J, Fu, Q, Wang, X, Shi, J, Zhang, W, Huang, Z, Zhang, B, 2011. Toward characterization of
2 the aerosol optical properties over Loess Plateau of Northwestern China. *Journal of Quantitative*
3 *Spectroscopy and Radiative Transfer* 112:346-360.
- 4 Chattopadhyay, G, Chakraborty, P, Chattopadhyay, S, 2012. Mann–Kendall trend analysis of tropospheric
5 ozone and its modeling using ARIMA. *Theoretical and Applied Climatology* 110:321-328.
- 6 Che, H, Wang, Y, Sun, J, Zhang, X, Zhang, X, Guo, J, 2013. Variation of Aerosol Optical Properties over
7 the Taklimakan Desert in China. *Aerosol and Air Quality Research* 13:777-785.
- 8 Chen, B, Yamada, M, Iwasaka, Y, Zhang, D, Wang, H, Wang, Z, Lei, H, Shi, G, 2015. Origin of
9 non-spherical particles in the boundary layer over Beijing, China: based on balloon-borne observations.
10 *Environmental Geochemistry and Health* 37:791-800.
- 11 Cheng, T, Chen, H, Gu, X, Yu, T, Guo, J, Guo, H, 2012. The inter-comparison of MODIS, MISR and
12 GOCART aerosol products against AERONET data over China. *Journal of Quantitative Spectroscopy and*
13 *Radiative Transfer* 113:2135-2145.
- 14 Chin, M, Diehl, T, Tan, Q, Prospero, J M, Kahn, R A, Remer, L A, Yu, H, Sayer, A M, Bian, H,
15 Geogdzhayev, I V, Holben, B N, Howell, S G, Huebert, B J, Hsu, N C, Kim, D, Kucsera, T L, Levy, R C,
16 Mishchenko, M I, Pan, X, Quinn, P K, Schuster, G L, Streets, D G, Strode, S A, Torres, O, Zhao, X P,
17 2014. Multi-decadal aerosol variations from 1980 to 2009: a perspective from observations and a global
18 model. *Atmos. Chem. Phys.* 14:3657-3690.
- 19 Christopher, S A, Gupta, P, Haywood, J, Greed, G, 2008. Aerosol optical thicknesses over North Africa: 1.
20 Development of a product for model validation using Ozone Monitoring Instrument, Multiangle Imaging
21 Spectroradiometer, and Aerosol Robotic Network. *Journal of Geophysical Research: Atmospheres*
22 113:n/a-n/a.
- 23 Diner, D J, Abdou, W A, Bruegge, C J, Conel, J E, Crean, K A, Gaitley, B J, Helmlinger, M C, Kahn, R A,
24 Martonchik, J V, Pilorz, S H, Holben, B N, 2001. MISR aerosol optical depth retrievals over southern
25 Africa during the SAFARI-2000 Dry Season Campaign. *Geophysical Research Letters* 28:3127-3130.
- 26 Diner, J C B, Terrence H. Reilly, Carol J. Bruegge, James E. Conel, Ralph A. Kahn., John V. Martonchik,
27 T P A, Roger Davies, Siegfried A. W. Gerstl, Howard R. Gordon., Jan-Peter Muller, R B M, Piers J.
28 Sellers, Bernard Pinty, and Michel M. Verstraete, 1998. Multi-angle Imaging SpectroRadiometer (MISR)
29 instrument description and experiment overview. *IEEE Transaction on Geoscience and Remote Sensing.*
30 *IEEE TRANSACTIONS ON GEOSCIENCE AND REMOTE SENSING* 34:1071-1085.
- 31 Edgell, 2006. *Arabian deserts: nature, origin, and evaluation.* Springer: Netherlands.
- 32 Floutsis, A A, Korras-Carraca, M B, Matsoukas, C, Hatzianastassiou, N, Biskos, G, 2016. Climatology and
33 trends of aerosol optical depth over the Mediterranean basin during the last 12 years (2002–2014) based on
34 Collection 006 MODIS-Aqua data. *Science of The Total Environment* 551–552:292-303.
- 35 Gherboudj, I G, Hosni, 2014. Spatiotemporal assessment of dust loading over the United Arab Emirates.
36 *International Journal of Climatology* 34:3321-3335.
- 37 Gilbert, R, 1987. *Statistical methods for environmental pollution monitoring.*
- 38 Hansen, J, Sato, M, Ruedy, R, Lacis, A, Oinas, V, 2000. Global warming in the twenty-first century: An
39 alternative scenario. *Proceedings of the National Academy of Sciences* 97:9875-9880.
- 40 Haywood, J, Boucher, O, 2000. Estimates of the direct and indirect radiative forcing due to tropospheric
41 aerosols: A review. *Reviews of Geophysics* 38:513-543.
- 42 He, Q, Zhang, M, Huang, B, 2016. Spatio-temporal variation and impact factors analysis of satellite-based
43 aerosol optical depth over China from 2002 to 2015. *Atmospheric Environment* 129:79-90.

44 Holben, B N, Eck, T F, Slutsker, I, Tanre, D, Buis, J P, Setzer, A, Vermote, E, Reagan, J A, Kaufman, Y J,
45 Nakajima, T, Lavenu, F, Jankowiak, I, Smirnov, A, 1998. AERONET - A federated instrument network
46 and data archive for aerosol characterization. *Remote Sensing of Environment* 66:1-16.
47 Hsu, N C, Gautam, R, Sayer, A M, Bettenhausen, C, Li, C, Jeong, M J, Tsay, S C, Holben, B N, 2012.
48 Global and regional trends of aerosol optical depth over land and ocean using SeaWiFS measurements
49 from 1997 to 2010. *Atmos. Chem. Phys.* 12:8037-8053.
50 Iwasaka, Y, Shi, G Y, Kim, Y S, Matsuki, A, Trochkin, D, Zhang, D, Yamada, M, Nagatani, T, Nagatani,
51 M, Shen, Z, Shibata, T, Nakata, H, 2004. Pool of dust particles over the Asian continent: Balloon-borne
52 optical particle counter and ground-based lidar measurements at Dunhuang, China. *Environmental*
53 *Monitoring and Assessment* 92:5-24.
54 Kahn, R, Petzold, A, Wendisch, M, Bierwirth, E, Dinter, T, Esselborn, M, Fiebig, M, Heese, B, Knippertz,
55 P, MÜLLer, D, Schladitz, A, Von Hoyningen-Huene, W, 2009. Desert dust aerosol air mass mapping in the
56 western Sahara, using particle properties derived from space-based multi-angle imaging. *Tellus B*
57 61:239-251.
58 Kahn, R A, Gaitley, B J, Garay, M J, Diner, D J, Eck, T F, Smirnov, A, Holben, B N, 2010. Multiangle
59 Imaging Spectroradiometer global aerosol product assessment by comparison with the Aerosol Robotic
60 Network. *Journal of Geophysical Research: Atmospheres* 115:n/a-n/a.
61 Kahn, R A, Gaitley, B J, Martonchik, J V, Diner, D J, Crean, K A, Holben, B, 2005. Multiangle Imaging
62 Spectroradiometer (MISR) global aerosol optical depth validation based on 2 years of coincident Aerosol
63 Robotic Network (AERONET) observations. *Journal of Geophysical Research: Atmospheres* 110:D10S04.
64 Kaufman, Y J, Tanré, D, Remer, L A, Vermote, E F, Chu, A, Holben, B N, 1997. Operational remote
65 sensing of tropospheric aerosol over land from EOS moderate resolution imaging spectroradiometer.
66 *Journal of Geophysical Research: Atmospheres* 102:17051-17067.
67 Kendall, M G, 1975. *Rank Correlation Methods*. Griffin, London.
68 Kim, Y S, Iwasaka, Y, Shi, G-Y, Shen, Z, Trochkin, D, Matsuki, A, Zhang, D, Shibata, T, Nagatani, M,
69 Nakata, H, 2003. Features in Number Concentration-Size Distributions of Aerosols in the Free Atmosphere
70 over the Desert Areas in the Asian Continent: Balloon-Borne Measurements at Dunhuang, China. *Water,*
71 *Air and Soil Pollution: Focus* 3:147-159.
72 Kosmopoulos, P G, Kaskaoutis, D G, Nastos, P T, Kambezidis, H D, 2008. Seasonal variation of columnar
73 aerosol optical properties over Athens, Greece, based on MODIS data. *Remote Sensing of Environment*
74 112:2354-2366.
75 Kumar, K R, Sivakumar, V, Yin, Y, Reddy, R R, Kang, N, Diao, Y, Adesina, A J, Yu, X, 2014. Long-term
76 (2003–2013) climatological trends and variations in aerosol optical parameters retrieved from MODIS over
77 three stations in South Africa. *Atmospheric Environment* 95:400-408.
78 Kumar, K R, Yin, Y, Sivakumar, V, Kang, N, Yu, X, Diao, Y, Adesina, A J, Reddy, R R, 2015. Aerosol
79 climatology and discrimination of aerosol types retrieved from MODIS, MISR and OMI over Durban
80 (29.88°S, 31.02°E), South Africa. *Atmospheric Environment* 117:9-18.
81 Levy, R C, Remer, L A, Kleidman, R G, Mattoo, S, Ichoku, C, Kahn, R, Eck, T F, 2010. Global evaluation
82 of the Collection 5 MODIS dark-target aerosol products over land. *Atmospheric Chemistry and Physics*
83 10:10399-10420.
84 Li, J, Carlson, B E, Dubovik, O, Laciš, A A, 2014. Recent trends in aerosol optical properties derived from
85 AERONET measurements. *Atmos. Chem. Phys.* 14:12271-12289.
86 Li, L, Yang, J, Wang, Y, 2015. Retrieval of High-Resolution Atmospheric Particulate Matter
87 Concentrations from Satellite-Based Aerosol Optical Thickness over the Pearl River Delta Area, China.
88 *Remote Sensing* 7:7914.
89 Li, Z, Xia, X, Cribb, M, Mi, W, Holben, B, Wang, P, Chen, H, Tsay, S-C, Eck, T F, Zhao, F, Dutton, E G,
90 Dickerson, R E, 2007. Aerosol optical properties and their radiative effects in northern China. *Journal of*
91 *Geophysical Research: Atmospheres* 112:n/a-n/a.
92 Liu, J, Xia, X, Li, Z, Wang, P, Min, M, Hao, W, Wang, Y, Xin, J, Li, X, Zheng, Y, Chen, Z, 2010.
93 Validation of multi-angle imaging spectroradiometer aerosol products in China. *Tellus B* 62:117-124.

94 Lyamani, H, Olmo, F J, Alcántara, A, Alados-Arboledas, L, 2006. Atmospheric aerosols during the 2003
95 heat wave in southeastern Spain I: Spectral optical depth. *Atmospheric Environment* 40:6453-6464.

96 Mann, H B, 1945. Nonparametric tests against trend. *Econometrica* 13:245-259.

97 Mehta, M, Singh, R, Singh, A, Singh, N, Anshumali, 2016. Recent global aerosol optical depth variations
98 and trends — A comparative study using MODIS and MISR level 3 datasets. *Remote Sensing of*
99 *Environment* 181:137-150.

100 Menon, S, Hansen, J, Nazarenko, L, Luo, Y, 2002. Climate Effects of Black Carbon Aerosols in China and
101 India. *Science* 297:2250-2253.

102 Miller, S D, Kuciauskas, A P, Liu, M, Ji, Q, Reid, J S, Breed, D W, Walker, A L, Mandoos, A A, 2008.
103 Haboob dust storms of the southern Arabian Peninsula. *Journal of Geophysical Research: Atmospheres*
104 113:n/a-n/a.

105 Mishchenko, M I, Geogdzhayev, I V, 2007. Satellite remote sensing reveals regional tropospheric aerosol
106 trends. *Opt. Express* 15:7423-7438.

107 Ogunjobi, K O, Kim, Y J, He, Z, 2003. Aerosol optical properties during Asian dust storm episodes in
108 South Korea. *Theoretical and Applied Climatology* 76:65-75.

109 Park, S-H, Panicker, A S, Lee, D-I, Jung, W-S, Jang, S-M, Jang, M, Kim, D, Kim, Y-W, Jeong, H, 2010.
110 Characterization of chemical properties of atmospheric aerosols over Anmyeon (South Korea), a super site
111 under Global Atmosphere Watch. *Journal of Atmospheric Chemistry* 67:71-86.

112 Prasad, A K, Singh, R P, 2007. Comparison of MISR-MODIS aerosol optical depth over the Indo-Gangetic
113 basin during the winter and summer seasons (2000-2005). *Remote Sensing of Environment* 107:109-119.

114 Sayer, A M, Hsu, N C, Bettenhausen, C, Jeong, M J, 2013. Validation and uncertainty estimates for
115 MODIS Collection 6 “Deep Blue” aerosol data. *Journal of Geophysical Research: Atmospheres*
116 118:7864-7872.

117 Sen, P K, 1968. Estimates of the Regression Coefficient Based on Kendall's Tau. *Journal of the American*
118 *Statistical Association* 63:1379-1389.

119 Shi, Y, Zhang, J, Reid, J S, Hyer, E J, Eck, T F, Holben, B N, Kahn, R A, 2011. A critical examination of
120 spatial biases between MODIS and MISR aerosol products: A application for potential AERONET
121 deployment. *Atmospheric Measurement Techniques (AMT) & Discussions (AMTD)*.

122 Smirnov, A, Holben, B N, Eck, T F, Dubovik, O, Slutsker, I, 2000. Cloud-Screening and Quality Control
123 Algorithms for the AERONET Database. *Remote Sensing of Environment* 73:337-349.

124 Tanré, D, Kaufman, Y J, Holben, B N, Chatenet, B, Karnieli, A, Lavenu, F, Blarel, L, Dubovik, O, Remer,
125 L A, Smirnov, A, 2001. Climatology of dust aerosol size distribution and optical properties derived from
126 remotely sensed data in the solar spectrum. *Journal of Geophysical Research: Atmospheres*
127 106:18205-18217.

128 Tesfaye, M, Sivakumar, V, Botai, J, Mengistu Tsidu, G, 2011. Aerosol climatology over South Africa
129 based on 10 years of Multiangle Imaging Spectroradiometer (MISR) data. *Journal of Geophysical Research:*
130 *Atmospheres* 116:n/a-n/a.

131 Tripathi, S N, Dey, S, Chandel, A, Srivastava, S, Singh, R P, Holben, B N, 2005. Comparison of MODIS
132 and AERONET derived aerosol optical depth over the Ganga Basin, India. *Ann. Geophys.* 23:1093-1101.

133 Wang, H, Zhang, L, Cao, X, Zhang, Z, Liang, J, 2013. A-Train satellite measurements of dust aerosol
134 distributions over northern China. *Journal of Quantitative Spectroscopy and Radiative Transfer*
135 122:170-179.

136 Xia, X, 2011. Variability of aerosol optical depth and Angstrom wavelength exponent derived from
137 AERONET observations in recent decades. *Environ. Res. Let* 6:044011.

138 Xiangao, X, Hongbin, C, Pucal, W, 2004. Aerosol properties in a Chinese semiarid region. *Atmospheric*
139 *Environment* 38:4571-4581.

140 Xiao, N, Shi, T, Calder, C A, Munroe, D K, Berrett, C, Wolfenbarger, S, Li, D, 2009. Spatial characteristics
141 of the difference between MISR and MODIS aerosol optical depth retrievals over mainland Southeast Asia.
142 *Remote Sensing of Environment* 113:1-9.

143 Yoon, J, von Hoyningen-Huene, W, Kokhanovsky, A A, Vountas, M, Burrows, J P, 2012. Trend analysis
144 of aerosol optical thickness and Ångström exponent derived from the global AERONET spectral
145 observations. *Atmos. Meas. Tech.* 5:1271-1299.
146 Yu, J, Che, H, Chen, Q, Xia, X, Zhao, H, Wang, H, Wang, Y, Zhang, X, Shi, G, 2015. Investigation of
147 Aerosol Optical Depth (AOD) and Ångström Exponent over the Desert Region of Northwestern China
148 Based on Measurements from the China Aerosol Remote Sensing Network (CARSNET). *Aerosol and Air*
149 *Quality Research* 15:2024-2036.
150 Yue, S, Pilon, P, Phinney, B, Cavadias, G, 2002. The influence of autocorrelation on the ability to detect
151 trend in hydrological series. *Hydrological Processes* 16:1807-1829.
152 Zhang, W, Zhuang, G, Huang, K, Li, J, Zhang, R, Wang, Q, Sun, Y, Fu, J S, Chen, Y, Xu, D, Wang, W,
153 2010. Mixing and transformation of Asian dust with pollution in the two dust storms over the northern
154 China in 2006. *Atmospheric Environment* 44:3394-3403.
155 Zhang, X Y, Gong, S L, Arimoto, R, Shen, Z X, Mei, F M, Wang, D, Cheng, Y, 2003. Characterization
156 and Temporal Variation of Asian Dust Aerosol from a Site in the Northern Chinese Deserts. *Journal of*
157 *Atmospheric Chemistry* 44:241-257.
158 Zhang Y, S Z B, 2010. Comparison of MODIS and MISR aerosol optical thickness over east-central China
159 (in Chinese). *Sci Meteorol Sin*, 30:48-54.

160

161

162

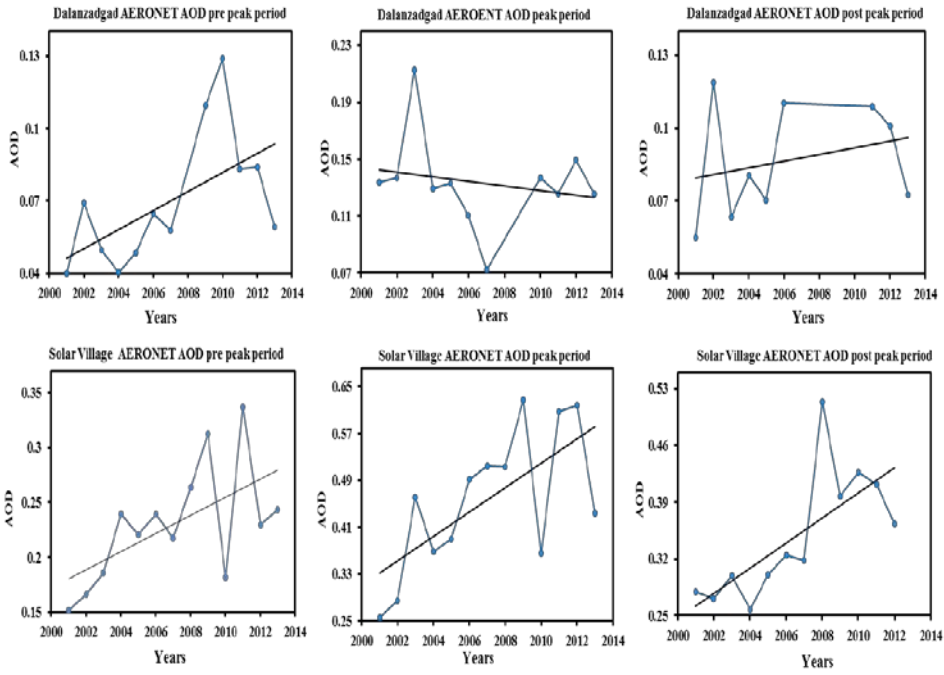
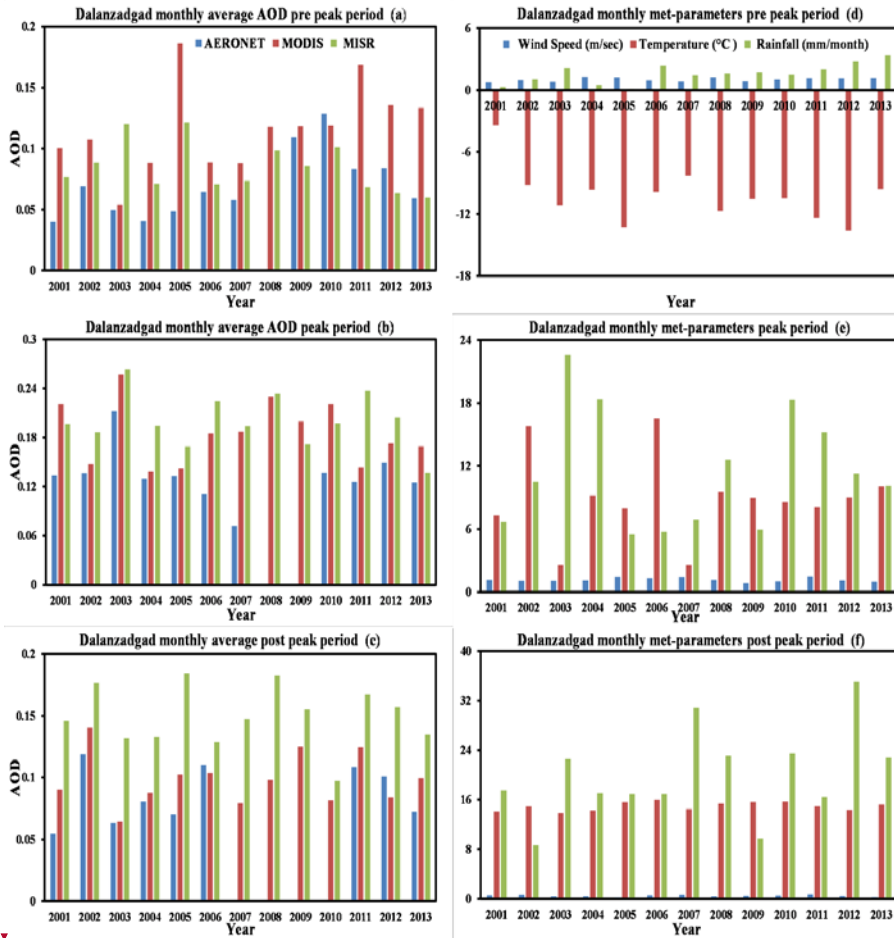


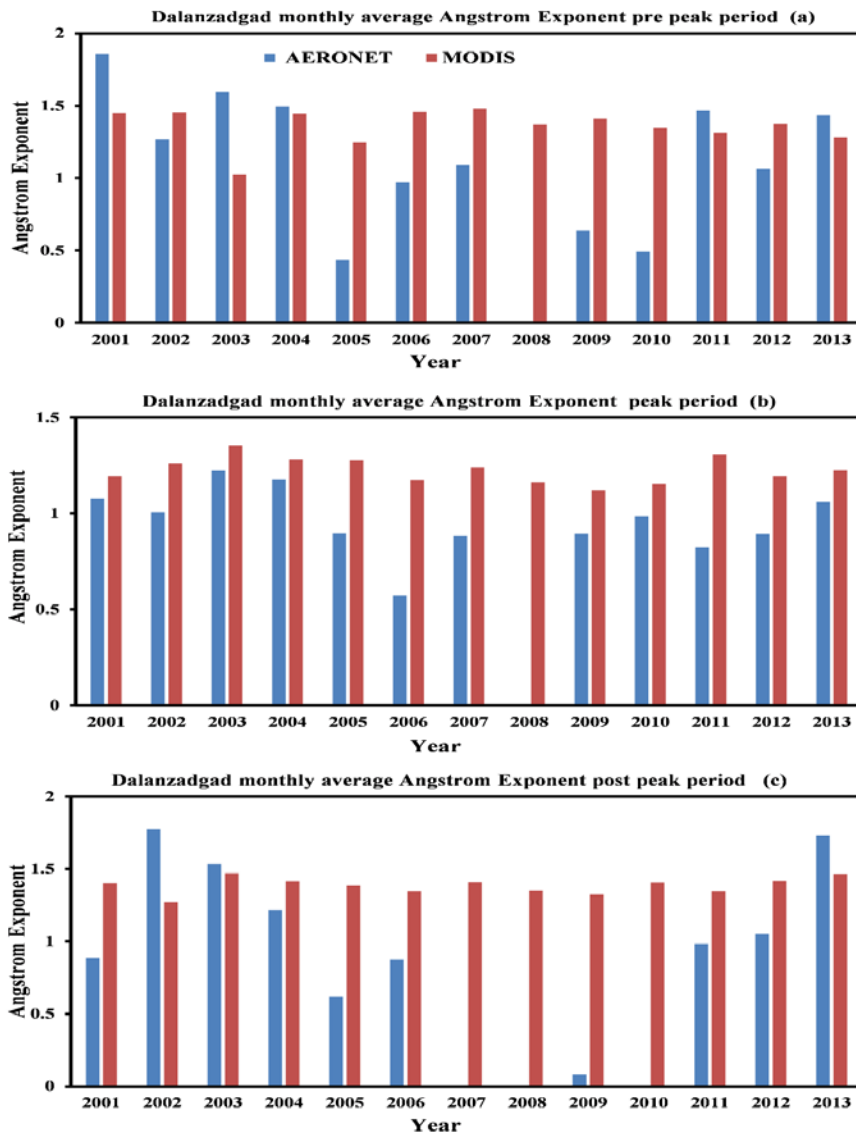
Fig. 1: Mann- Kendall trend of AERONET AOD in Dalanzadgad and Solar Village from 2001-2013

163
 164
 165
 166
 167
 168
 169
 170

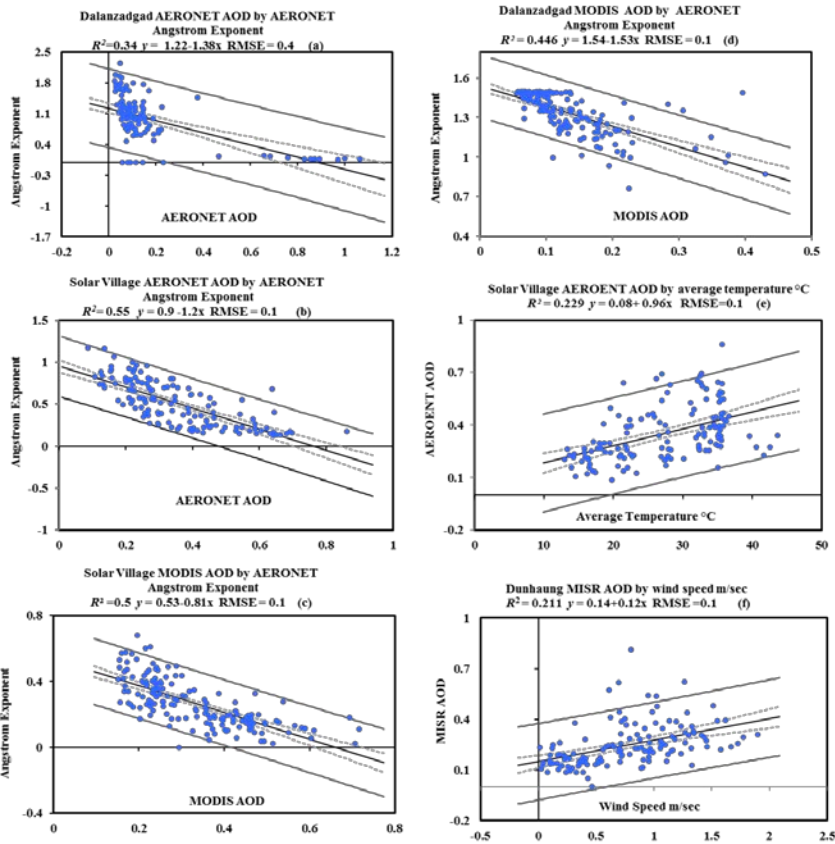


171
 172 Fig. 2 - (a) – (f) AOD Variability in Dalanzadgad retrieved from AERONET, MODIS and MISR from
 173 2001-2013 and monthly mean Meridional wind speed m/sec, average temperature and total rainfall mm/month
 174 in Dalanzadgad in pre/post peak period

Deleted: ¶



176
 177 Fig. 3 (a) – (c) Angstrom Exponent Variability in Dalanzadgad retrieved from AERONET and MODIS from
 178 2001-2013 for pre peak, peak and post peak period



179
180

181 Fig.4 Regression between (a) Dalanzadgad AERONET AOD by AERONET Angstrom (b) Dalanzadgad
182 MODIS AOD by AERONET Angstrom in Dalanzadgad (c) Solar Village AERONET AOD by AERONET
183 Angstrom Exponent (d) Solar village AERONET AOD by average temperature (e) Solar Village MODIS AOD
184 by AEROENT Angstrom Exponent (f) Dunhuang MISR AOD by wind speed.

185
186
187
188
189
190

Table 1: Trend of Aerosol Optical Depth using Aeronet data over a period of 2001 -2013

Dalangzadgad Year 2001 – 2013	AERONET AOD (550nm) Pre Peak Period	AERONET AOD (550nm) Peak Period	AERONET (550nm) Post Peak Period

213
214
215
216
217
218
219
220
221
222
223
224
225
226
227

<i>P</i> Value	0.045 < 0.05	0.445 > 0.05	0.612 > 0.05
Sen's Slope Value	0.004 € (0.003,0.005)	-0.001 € (-0.001, 0.001)	0.003 € (0.004, 0.006)
Null Hypothesis	Rejected	Accepted	Accepted
Solar Village Year 2001 – 2013	AERONET AOD (550nm) Pre Peak Period	AERONET AOD (550nm) Peak Period	AERONET (550nm) Post Peak Period
<i>P</i> Value	0.022 < 0.05	0.015 < 0.05	0.005 < 0.05
Sen's Slope Value	0.012 € (0.011,0.014)	0.025 € (0.023,0.028)	0.014 € (0.013, 0.015)
Null Hypothesis	Rejected	Rejected	Rejected

Table 2: Trend of Aerosol Optical Depth using MODIS data over a period of 2001 -2013

Dalangzadgad Year 2001 – 2013	MODIS AOD (550nm) Pre Peak Period	MODIS AOD (550nm) Peak Period	MODIS AOD (550nm) Post Peak Period
<i>P</i> Value (Two Tailed)	0.031 < 0.05	0.841 > 0.05	0.947 > 0.05
Sen's Slope Value	0.006 € (0.005, 0.006)	0 € (0, 0.002)	0.0012 € (-0, 0.001)
Null Hypothesis	Rejected	Accepted	Accepted
Dunhuang Year 2001 – 2013	MODIS AOD (550nm) Pre Peak Period	MODIS AOD (550nm) Peak Period	MODIS AOD (550nm) Post Peak Period

228
229
230
231
232
233
234
235

<i>P</i> Value	0.492 > 0.05	0.000 < 0.05	0.086 > 0.05
Sen's Slope Value	0.002 ∉ (-0.011, -0.012)	-0.011 ∈ (0.002, 0.003)	-0.008 ∉ (-0.007, -0.008)
Null Hypothesis	Accepted	Rejected	Accepted
Solar Village Year 2001 – 2013	MODIS AOD (550nm) Pre Peak Period	MODIS AOD (550nm) Peak Period	MODIS AOD (550nm) Post Peak Period
<i>P</i> Value	0.153 > 0.05	0.045 < 0.05	0.028 < 0.05
Sen's Slope Value	0.002 ∉ (0.002, 0)	0.015 ∈ (0.013, 0.017)	0.008 ∉ (0.007, 0.008)
Null Hypothesis	Accepted	Rejected	Rejected

Table 3: Trend of Aerosol Optical Depth using MISR data over a period of 2001 -2013

Dalangzadgad Year 2001 – 2013	AOD (555nm) Pre Peak Period	AOD (555nm) Peak Period	AOD (555nm) Post Peak Period
<i>P</i> Value (Two Tailed)	0.063 > 0.05	0.947 > 0.05	0.947 > 0.05
Sen's Slope Value	-0.003 ∉ (-0.002, -0.003)	-0.001 ∉ (-0.003, 0.001)	-7.973E-4 (-0.001, 0.000)
Null Hypothesis	Accepted	Accepted	Accepted
Dunhuang Year 2001 – 2013	AOD (555nm nm) Pre Peak Period	AOD (555nm nm) Peak Period	AOD (555nm nm) Post Peak Period
<i>P</i> Value	0.459 > 0.05	0.153 > 0.05	0.311 > 0.05
Sen's Slope Value	0.004 ∉ (0.004, 0.005)	-0.013 ∈ (-0.011, -0.015)	-0.003 ∈ (-0.002, -0.004)

Null Hypothesis	Accepted	Accepted	Accepted
Solar Village Year 2001 – 2013	AOD (555nm) Pre Peak Period	AOD (555nm) Peak Period	AOD (555nm) Post Peak Period
<i>P</i> Value	0.197 > 0.05	0.063 > 0.05	0.381 > 0.05
Sen's Slope Value	0.003 ∉ (0.003, 0.003)	0.012 ∉ (0.010, 0.013)	0.006 ∉ (0.003, 0.006)
Null Hypothesis	Accepted	Accepted	Accepted

236
237
238
239
240
241
242
243
244
245
246

Table 4: Trend of AERONET Angstrom Exponent 440-879 using AERONET data over a period of 2001 -2013

Dalangzadgad Year 2001 – 2013	AERONET Angstrom Exponent 440-870 Pre Peak Period	AERONET Angstrom Exponent 440-870 Peak Period	AERONET Angstrom Exponent 440-870 Post Peak Period
<i>P</i> Value (Two Tailed)	0.20 > 0.05	0.197 > 0.05	0.8 > 0.05
Sen's Slope Value	-0.071 ∉ (0.034-0.062)	-0.016 ∉ (-0.016,0.018)	-0.006 ∉ (-0.001 , -0.035)
Null Hypothesis	Accepted	Accepted	Accepted
Solar Village Year 2001 – 2013	AERONET Angstrom Exponent 440-870 Pre Peak Period	AERONET Angstrom Exponent 440-870 Peak Period	AERONET Angstrom Exponent 440-870 Post Peak Period
<i>P</i> Value	0.2 > 0.05	0.1 > 0.05	0.1 > 0.05
Sen's Slope Value	-0.009 ∉ (-0.001, -0.007)	-0.009 ∉ (-0.010, -0.018)	-0.018 ∉ (-0.016, -0.018)

247
248
249
250
251
252
253

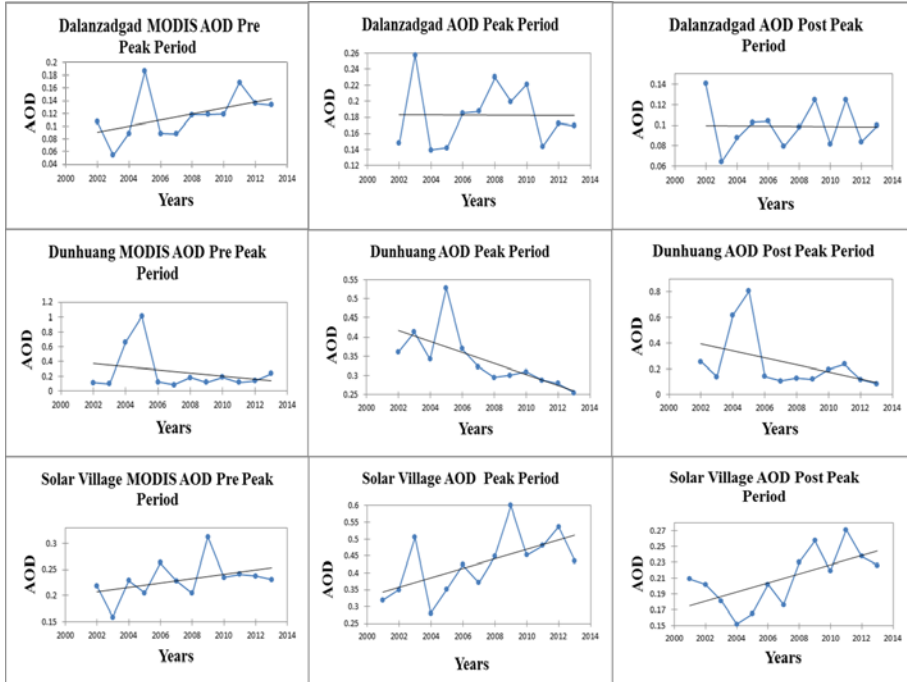
Null Hypothesis	Accepted	Accepted	Accepted
-----------------	----------	----------	----------

Table 5: Trend of MODIS Angstrom Exponent 540-870 over a period of 2001 -2013

Dalangzadgad Year 2001 – 2013	Angstrom Exponent (580-870) Monthly Average Pre Peak Period	Angstrom Exponent (580-870) Monthly Average Pre Peak Period	Angstrom Exponent (580-870) Monthly Average Pre Peak Period
<i>P</i> Value	0.459 > 0.05	0.153 > 0.05	0.638 > 0.05
Sen,s Slope Value	-0.011 € (-0.008 , -0.013)	-0.008 € (-0.006 , -0.011)	0.003
Null Hypothesis	Accepted	Accepted	Accepted
Dunhuang Year 2001 – 2013	Angstrom Exponent (580-870) Monthly Average Pre Peak Period	Angstrom Exponent (580-870) Monthly Average Pre Peak Period	Angstrom Exponent (580-870) Monthly Average Pre Peak Period
<i>P</i> Value	0.04 < 0.05	0.582 > 0.05	0.783 > 0.05
Sen,s Slope Value	0.023 € (0.020, 0.024)	0.004 € (0.003, 0.006)	0.006 € (0.001, 0.008)
Null Hypothesis	Rejected	Accepted	Accepted
Solar Village Year 2001 – 2013	Angstrom Exponent (580-870) Monthly Average Pre Peak Period	Angstrom Exponent (580-870) Monthly Average Pre Peak Period	Angstrom Exponent (580-870) Monthly Average Pre Peak Period
<i>P</i> Value	0.014 < 0.05	0.014 < 0.05	0.947 > 0.05
Sen,s Slope Value	-0.012 € (-0.010 , -0.013)	-0.012 € (-0.010, -0.013)	0.0009 € (- 0.010, 0.001)
Null Hypothesis	Rejected	Rejected	Accepted

254
255
256
257

258
259
260
261



262
263
264
265
266
267
268
269
270
271
272
273
274
275

Fig S1: Mann-Kendall trend of MODIS AOD in Dalanzadgad, Dunhuang and Solar Village from 2001-2013

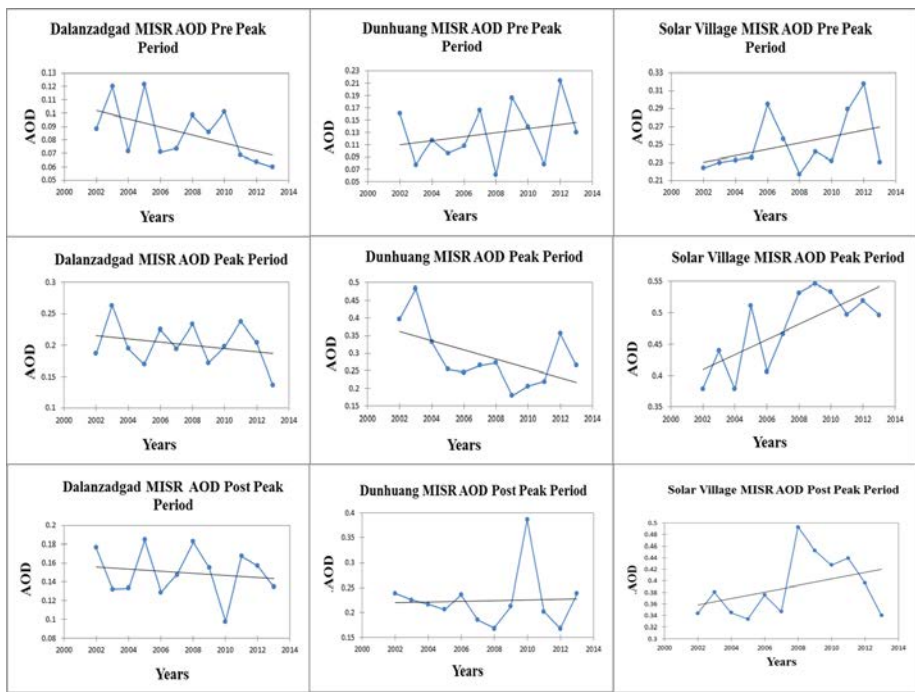


Fig S 2: Mann-Kendall trend of MISR AOD in Dalanzadgad, Dunhuang and Solar Village from 2001-2013

276
 277
 278
 279
 280
 281
 282
 283
 284
 285
 286
 287
 288
 289

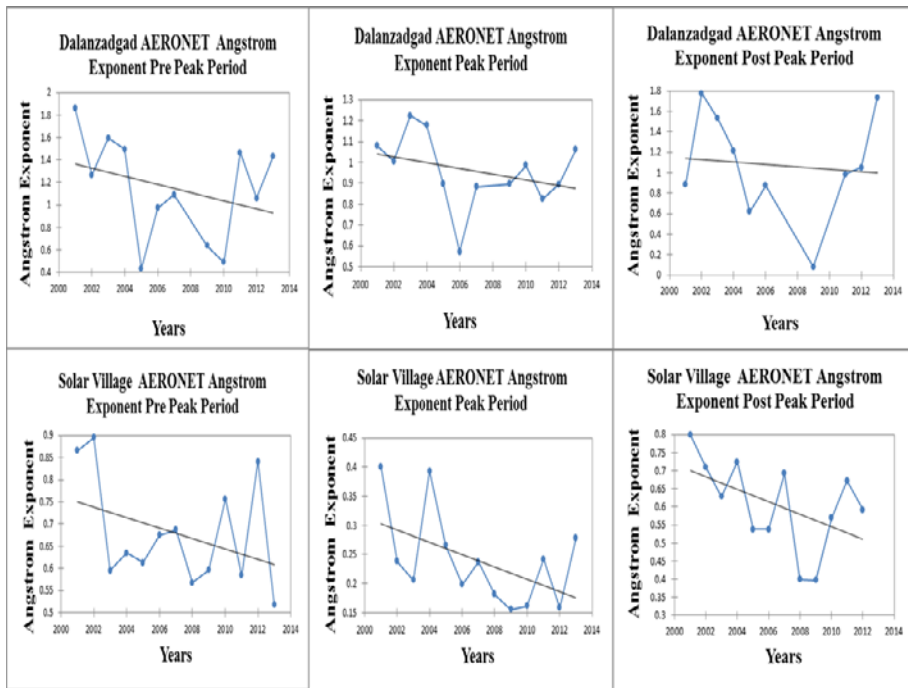


Fig S 3 : Mann- Kendall trend of AERONET Angstrom Exponent in Dalanzadgad, and Solar Village from 2001-2013

290
 291
 292
 293
 294
 295
 296
 297
 298
 299
 300
 301
 302
 303

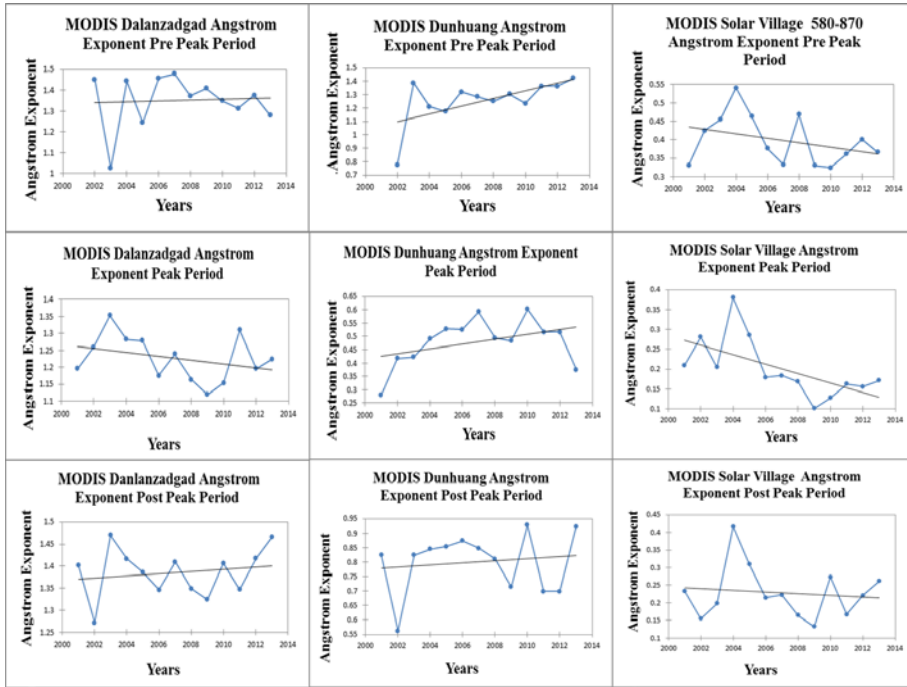


Fig S 4: Mann- Kendall trend of MODIS Angstrom Exponent in Dalanzadgad, Dunhuang and Solar Village from 2001-2013

304
 305
 306
 307
 308
 309
 310
 311
 312
 313
 314
 315
 316
 317
 318
 319
 320
 321

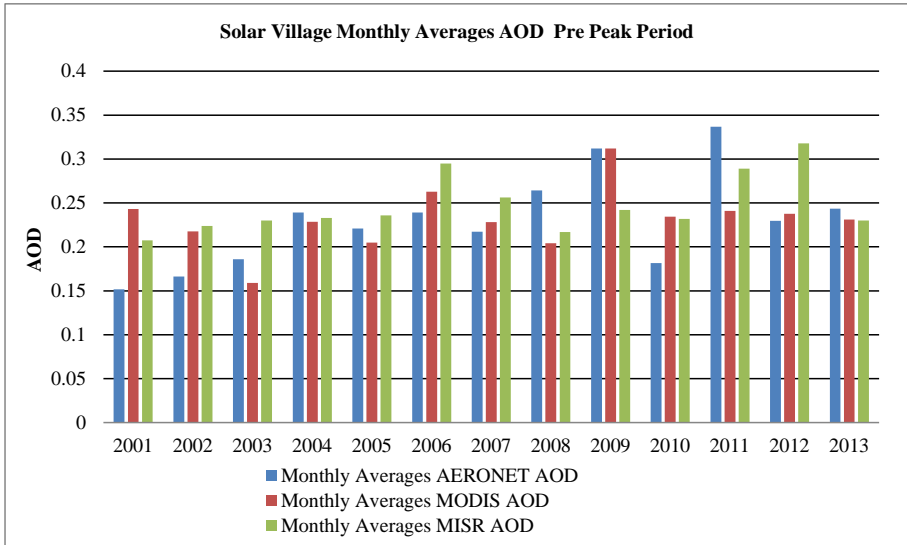
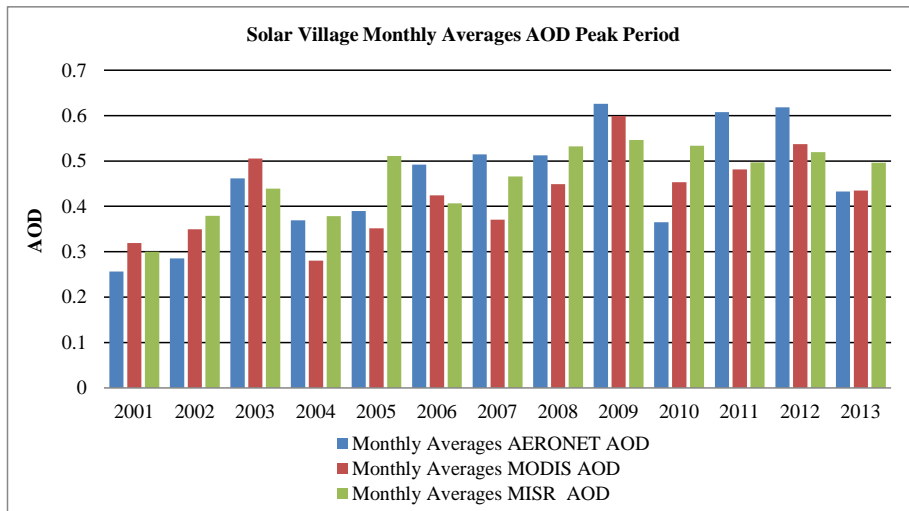


Fig S 5 (a): AOD Variability in Solar Village retrieved from AERONET, MODIS and MISR from 2001-2013 in pre peak period

322
 323
 324
 325
 326
 327
 328
 329
 330
 331
 332
 333
 334
 335
 336
 337
 338
 339



340 Fig S 5 (b): AOD Variability in Solar Village retrieved from AERONET, MODIS and MISR from
 341 2001-2013 in peak period
 342
 343
 344
 345
 346
 347
 348
 349
 350
 351
 352
 353
 354
 355
 356

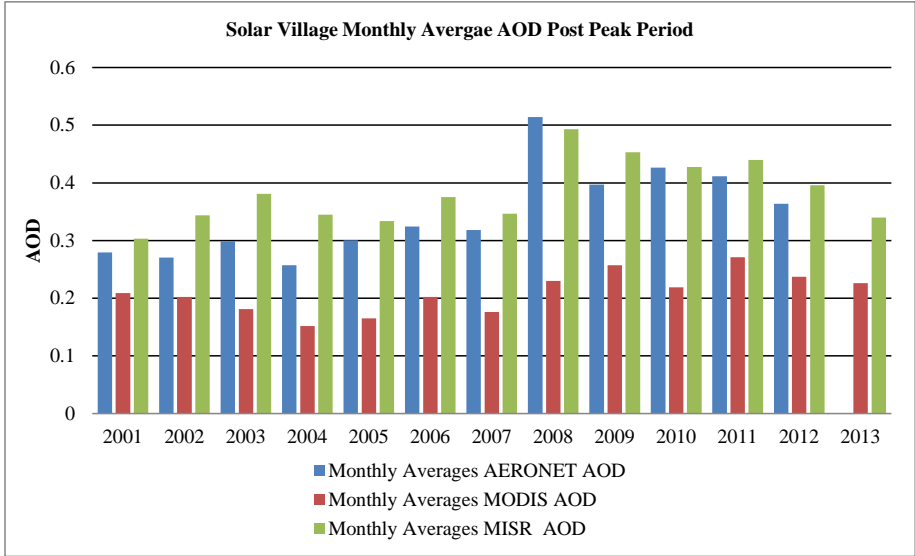


Fig S 5 (c): AOD Variability in Solar Village retrieved from AERONET, MODIS and MISR from 2001-2013 in post peak period

357
 358
 359
 360
 361
 362
 363
 364
 365
 366
 367
 368
 369
 370
 371
 372
 373

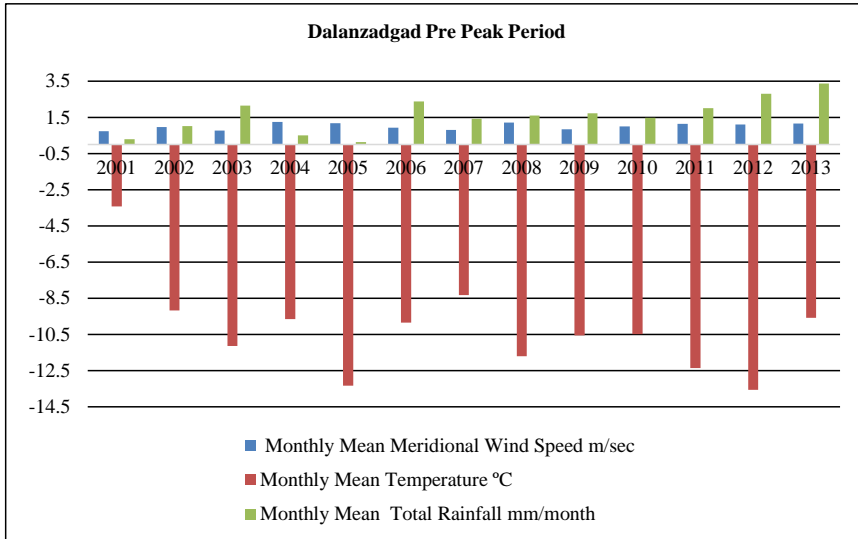


Fig S 5 (d): Monthly mean Meridional wind speed m/sec, Average Temperature and Total Rainfall mm/month in Solar Village in pre peak period

374
 375
 376
 377
 378
 379
 380
 381
 382
 383
 384
 385
 386
 387
 388
 389
 390
 391

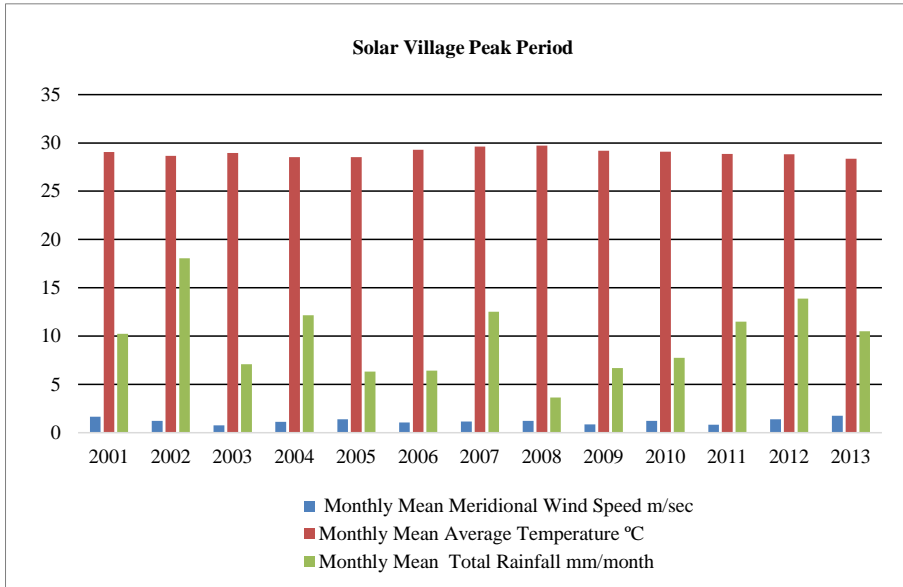


Fig S 5 (e): Monthly mean Meridional wind speed m/sec, Average Temperature and Total Rainfall mm/month in Solar Village in peak period

392
 393
 394
 395
 396
 397
 398
 399
 400
 401
 402
 403
 404
 405
 406
 407
 408

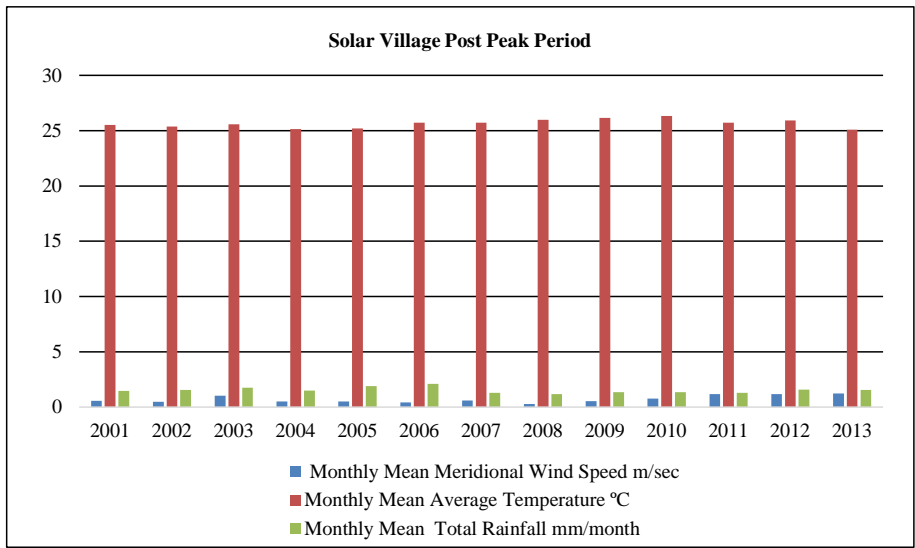
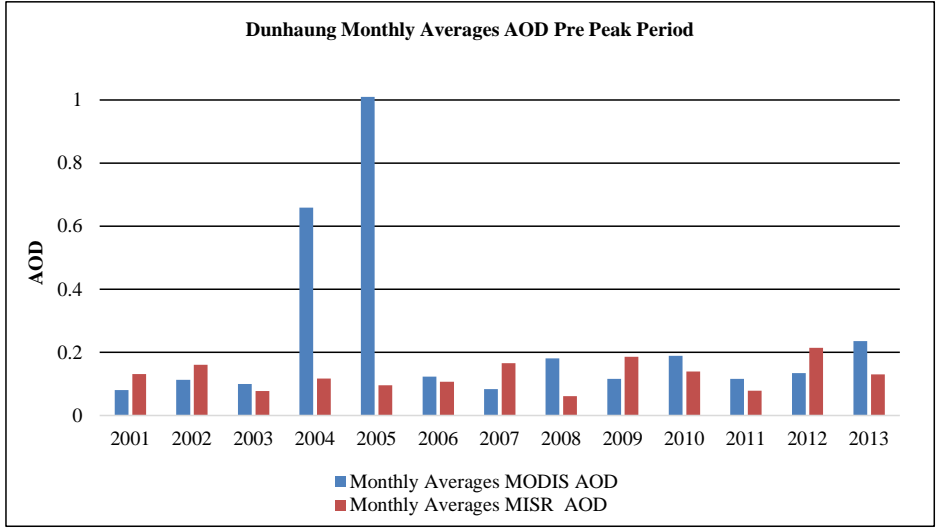


Fig S 5 (f): Monthly mean Meridional wind speed m/sec, Average Temperature and Total Rainfall mm/month in Solar Village in post peak period

409
 410
 411
 412
 413
 414
 415
 416
 417
 418
 419
 420
 421
 422
 423
 424
 425
 426



427
 428
 429
 430
 431
 432
 433
 434
 435
 436
 437
 438
 439
 440
 441
 442
 443
 444
 445

Fig S 6 (a): AOD Variability in Dunhuang retrieved from MODIS and MISR from 2001-2013 for pre peak period

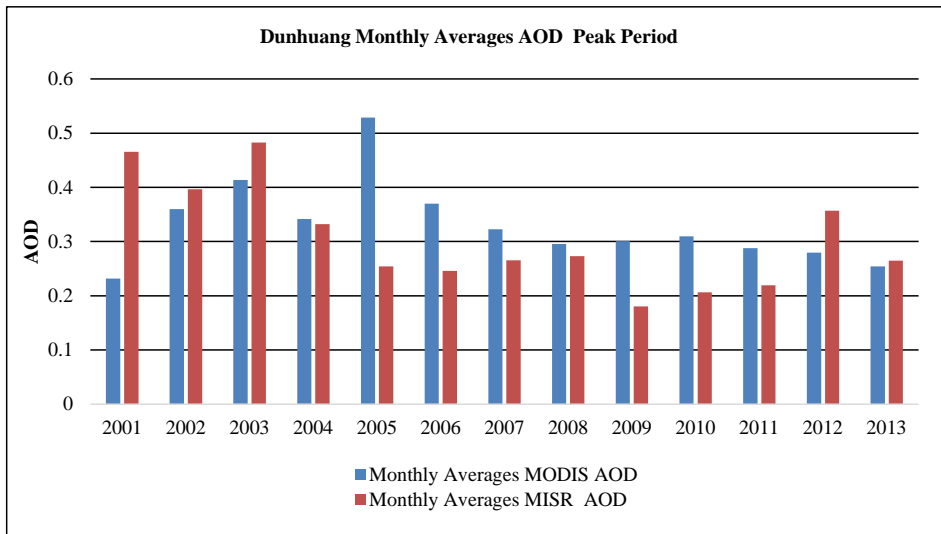
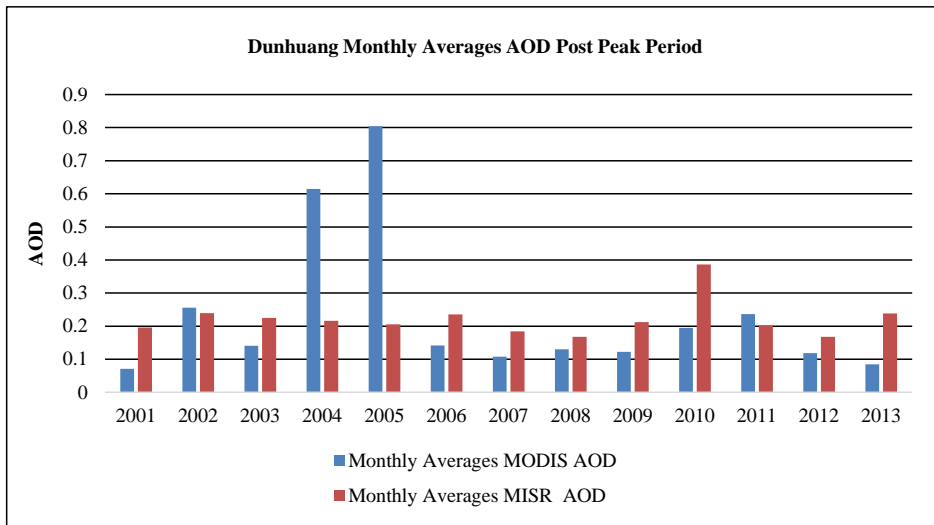


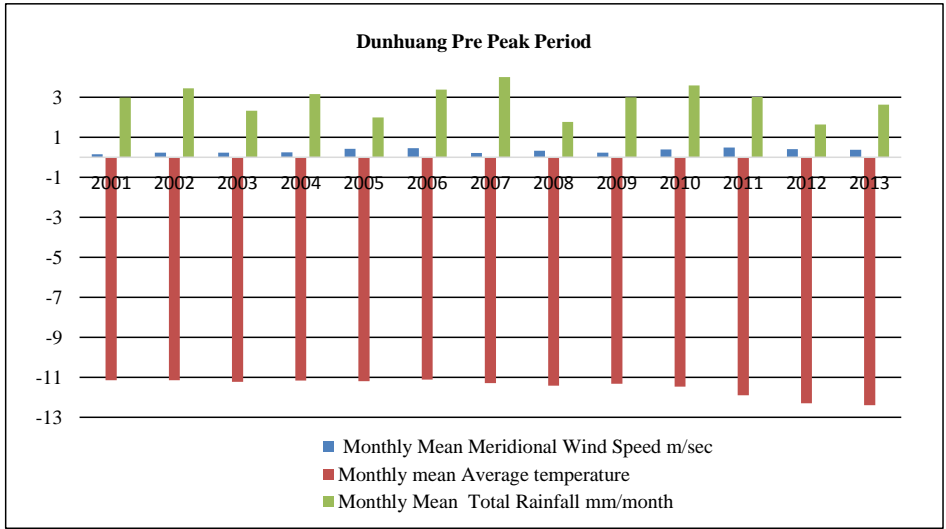
Fig S 6 (b): AOD Variability in Dunhuang retrieved from MODIS and MISR from 2001-2013 for peak period

446
 447
 448
 449
 450
 451
 452
 453
 454
 455
 456
 457
 458
 459
 460
 461
 462



463 Fig S 6 (c): AOD Variability in Dunhuang retrieved from MODIS and MISR from 2011-2013 for post peak
 464 period
 465

466
 467
 468
 469
 470
 471
 472
 473
 474
 475
 476
 477
 478
 479
 480
 481
 482
 483



484 Fig S 6 (d): Monthly mean Meridional wind speed m/sec, Average Temperature and Total Rainfall mm/month in
 485 Solar Village in pre peak period
 486

487
 488
 489
 490
 491
 492
 493
 494
 495
 496
 497
 498

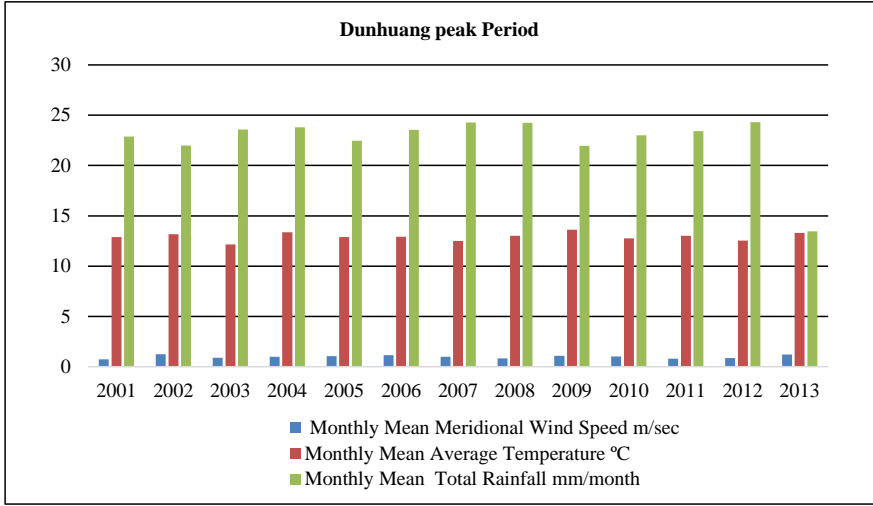


Fig S 6 (e): Monthly mean Meridional wind speed m/sec, Average Temperature and Total Rainfall mm/month in Solar Village in peak period

499
 500
 501
 502
 503
 504
 505
 506
 507
 508
 509
 510
 511
 512
 513

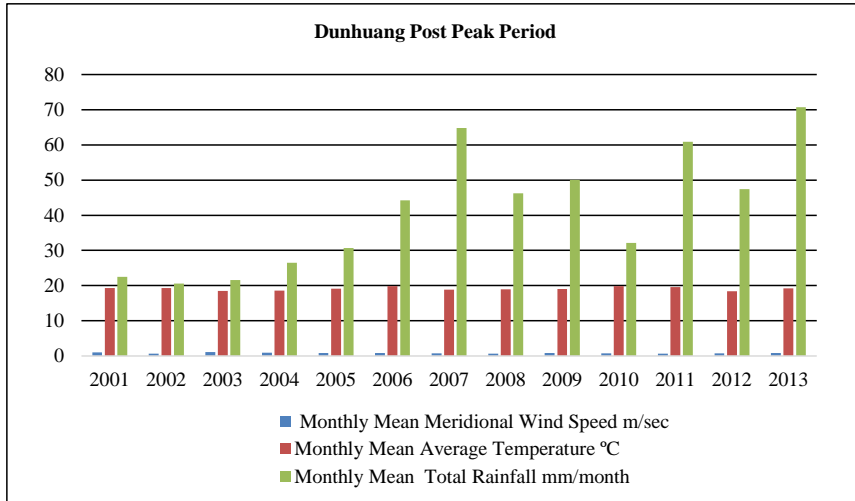
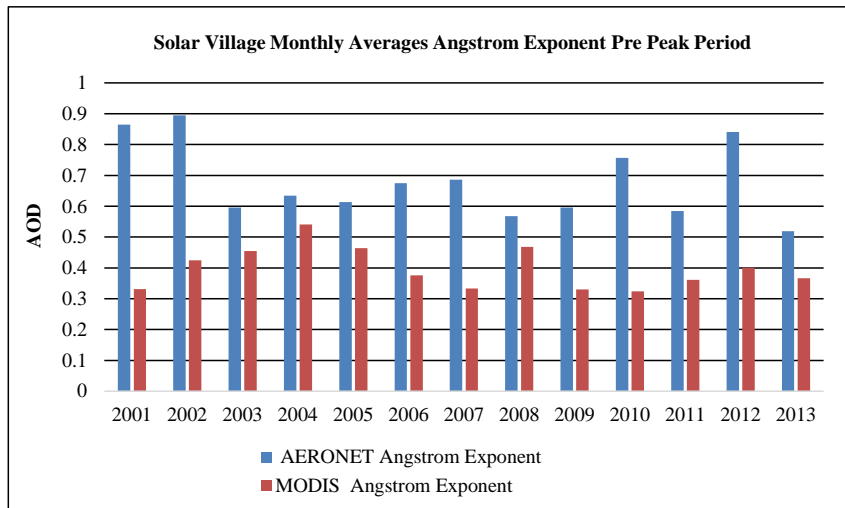


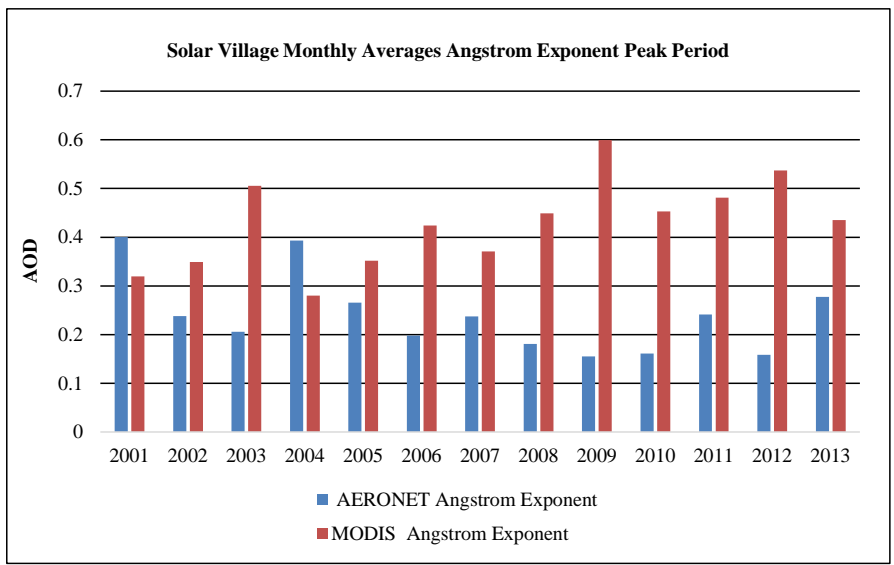
Fig S 6 (f): Monthly mean Meridional wind speed m/sec, Average Temperature and Total Rainfall mm/month in Solar Village in post peak period

514
 515
 516
 517
 518
 519
 520
 521
 522
 523
 524
 525
 526
 527
 528
 529
 530
 531
 532
 533
 534



535
 536 Fig. S 7 (a): Angstrom Exponent Variability in Solar Village retrieved from AERONET and MODIS from
 537 2001-2013 for pre peak period
 538

539
 540
 541
 542
 543
 544
 545
 546
 547
 548
 549
 550



551 Fig. S 7 (b): Angstrom Exponent Variability in Solar Village retrieved from AERONET and MODIS from
 552 2001-2013 for peak period
 553

554
 555
 556
 557
 558
 559
 560
 561
 562
 563
 564
 565
 566
 567
 568
 569

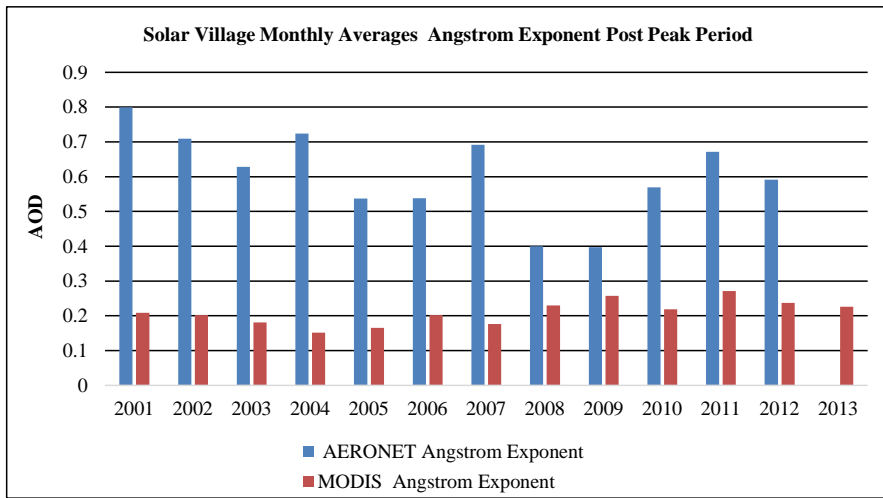
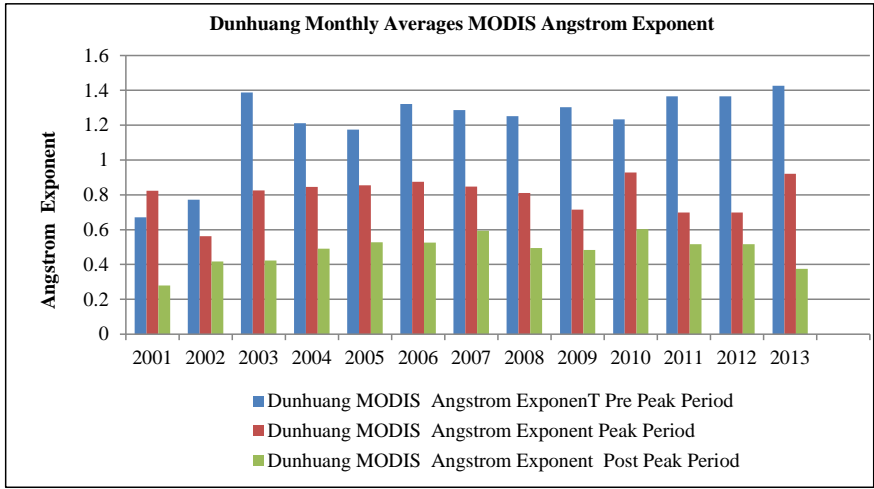


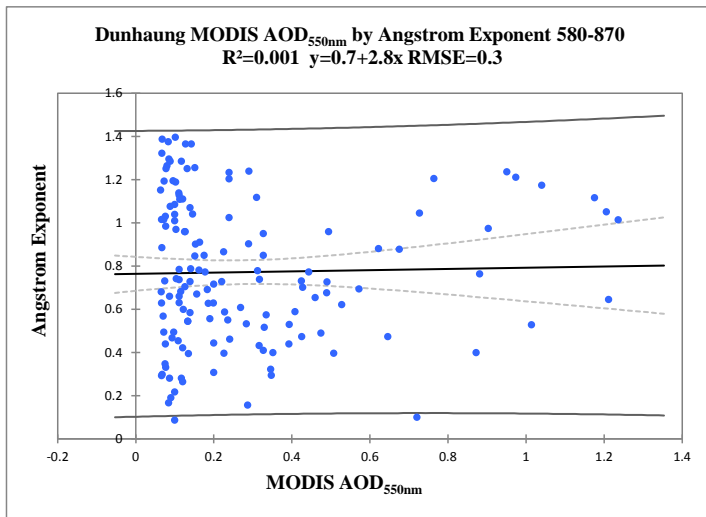
Fig. S 7 (c): Angstrom Exponent Variability in Solar Village retrieved from AERONET and MODIS from 2001-2013 for post peak period

570
 571
 572
 573
 574
 575
 576
 577
 578
 579
 580
 581
 582
 583
 584
 585
 586
 587
 588
 589

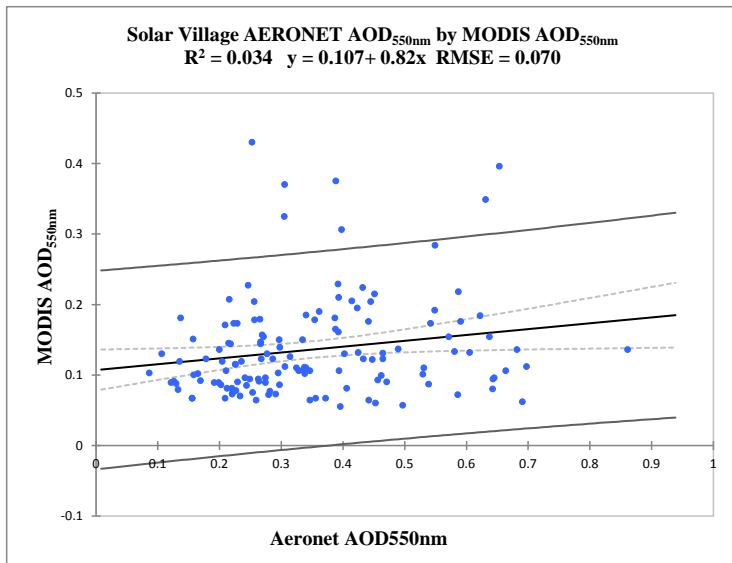


590
591
592
593
594
595
596
597
598
599
600
601
602
603
604
605
606
607
608
609

Fig S 8: Monthly averages of Angstrom Exponent variability in Dunhuang retrieved from MODIS for the years of 2001-2013 over difference wavelengths in study periods are shown in this figure



610
 611 Fig S 9 (a): Regression between MODIS AOD against Angstrom Exponent (α) 580-870 in Dunhuang
 612
 613



614
 615 Fig S 9 (b): Regression between Aeronet AOD against MODIS AOD in Solar Village
 616

617
618
619

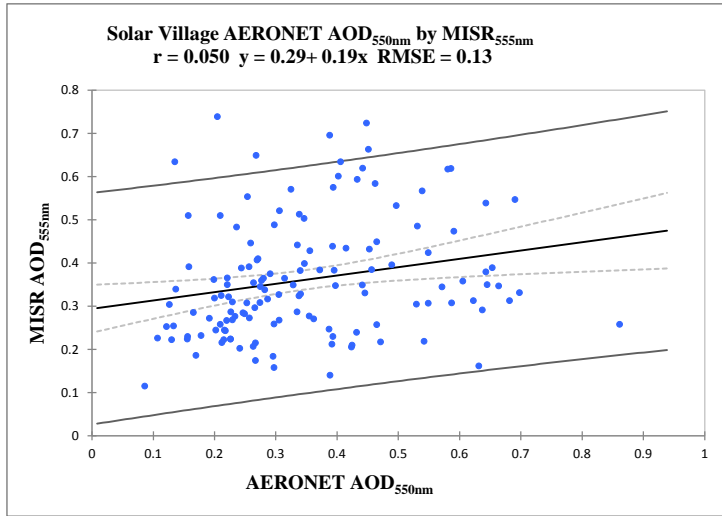


Fig S 9 (c): Regression between Aeronet AOD against MISR AOD in Solar Village

620
621
622
623

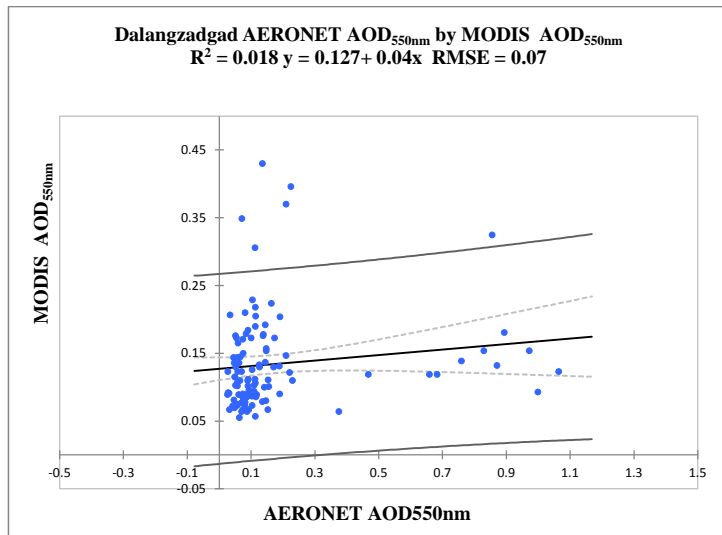


Fig S 9 (d): Regression between Aeronet AOD against MODIS AOD in Dalangzadgad

624
625
626

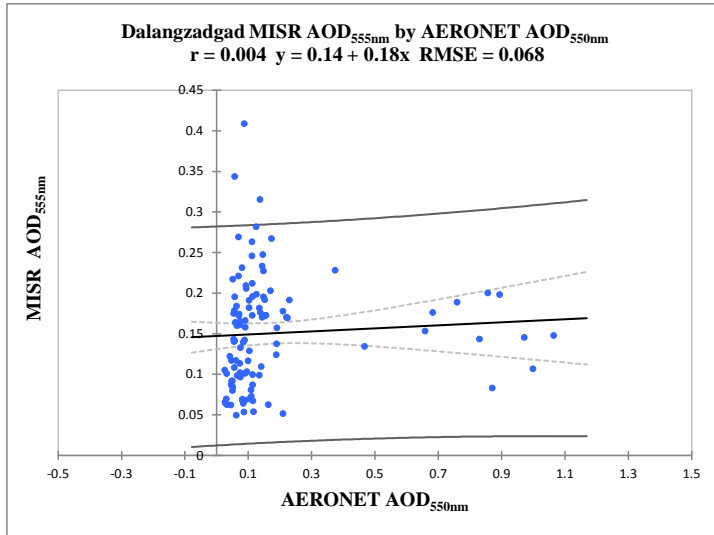


Fig S 9 (e): Regression between Aeronet AOD against MODIS AOD in Dalangzadgad

627
628

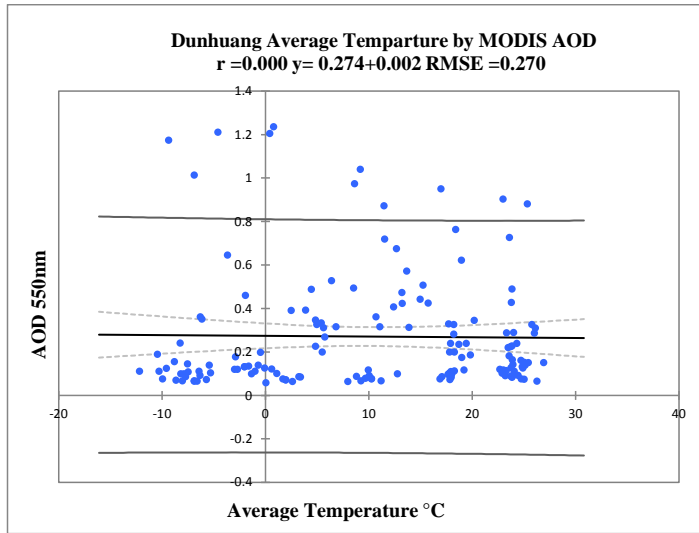


Fig S 9 (f): Regression between MODIS AOD against Average Temperature °C in Dunhuang

629
630
631
632

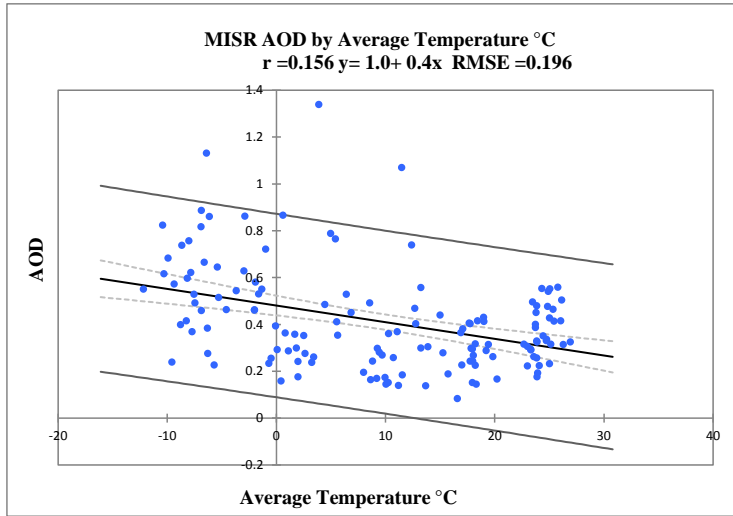


Fig S 9 (g): Regression between MISR AOD against Average Temperature °C in Dunhuang

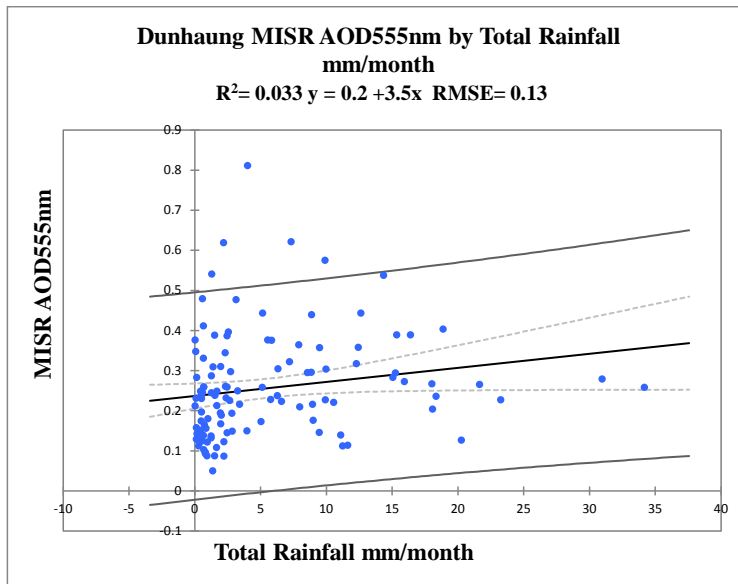


Fig S 9 (h): Regression between MISR AOD against Total Rainfall in Dunhuang

633
634
635
636
637
638

639
640
641